

DIPLOMA THESIS

# MODELLING OF CASSINI LANGMUIR PROBE MEASUREMENTS

THOMAS NILSSON

Swedish Institute of Space Physics  
Uppsala, Sweden

OCTOBER 13, 2009

## **Abstract**

On board the Cassini spacecraft, which is currently in orbit around the outer planet Saturn, a Langmuir probe instrument measures the various plasmas surrounding the planet and its moons. This instrument consist of a sphere, (and connecting parts to the spacecraft), and it's charged to different potentials relative to the spacecraft while the current flow is measured. Then from these measurements different plasma parameters can be determined, giving valuable information about the Saturn system. These measurments will however be affected by the plasma potential surrounding the spacecraft as well as the various parts of the instruments itself. The model currently used assumes that the instrument is a perfect sphere without anything connected to it.

In order to understand how, and to what extent, this will be affecting the measurements simulations has been performed with the SPIS software. Firstly the influence of the Cassini spacecraft itself was investigated, for various plasmas similar to those found around Saturn and its moons.

Then, the influence of one of these connecting parts (the "stub") on the measurements was investigated by simulating the current flow to the Langmuir probe for two plasmas. One plasma with short Debye length and one with longer Debye length, both of which can be found at different locations around Saturn and its moons.

It has been found that the presence of the stub decreases the current measured by the Langmuir probe by 3 to 8 percent and that this effect is most prominnet with shorter Debye length.

# Acknowledgments

First of all I would like to recognise my great supervisor Dr Anders Eriksson of the Swedish institute for space physics, Uppsala division (IRFU) without whom this report would not have been possible.

I would like to give thanks to Simon Clucas and David Rogers, both working at ESA/ESTEC in Noordwijk, The Netherlands, for their much needed assistance and for taking the time to meet with Alexander Sjögren and myself during our visit to ESTEC.

And a big greeting to the rest of IRFU for making my time here at the institute very pleasant and joyful, (with barbecue, restaurant visits, movie evenings etcetera).

Last but not least I would also like to thank Alexander Sjögren, Madeleine Holmberg and Marco Chiaretta for their pleasant company during all of our lunch meetings and *fika*.

# Contents

<b>Acknowledgements</b>	<b>i</b>
<b>1 Space and plasma</b>	<b>1</b>
1.1 Introduction . . . . .	1
1.2 Plasma parameters . . . . .	2
<b>2 Cassini-Huygens Spacecraft</b>	<b>3</b>
2.1 Introduction . . . . .	3
2.2 The Cassini orbiter . . . . .	3
<b>3 The Langmuir probe</b>	<b>5</b>
3.1 The instrument . . . . .	5
3.2 Probe theory . . . . .	5
<b>4 Spacecraft plasma interaction system, (SPIS)</b>	<b>9</b>
4.1 Introduction . . . . .	9
4.2 Model of Cassini . . . . .	9
4.3 Model of the Langmuir probe . . . . .	10
<b>5 Results of Cassini simulations</b>	<b>12</b>
5.1 Introduction . . . . .	12
5.2 Results . . . . .	13
<b>6 Results of Langmuir probe simulations</b>	<b>17</b>
6.1 Introduction . . . . .	17
6.2 Low density $1 \text{ cm}^{-3}$ and high temperature 1 eV . . . . .	17
6.3 High density $1,000 \text{ cm}^{-3}$ and low temperature 0.05 eV . . . . .	21
<b>7 Conclusions and outlook</b>	<b>25</b>
7.1 Conclusions . . . . .	25
7.2 Outlook . . . . .	25
<b>Bibliography</b>	<b>28</b>
<b>A Appendix: Simulations with SPIS</b>	<b>29</b>
A.1 Prior to beginning the simulations . . . . .	29
A.2 Building the model . . . . .	30
A.3 Running SPIS . . . . .	30

A.4	Taking care of the results . . . . .	34
<b>B</b>	<b>Appendix: Models used</b>	<b>36</b>
B.1	Cassini model . . . . .	36
B.2	Langmuir probe model . . . . .	43
<b>C</b>	<b>Appendix: List of simulations</b>	<b>47</b>

# Chapter 1

## Space and plasma

### 1.1 Introduction

Interplanetary space is not an absolute vacuum, as no such thing can exist in nature, but is in fact filled with a gas with very low density. It has such a low density that compared to anything on Earth it can in most applications be approximated with a vacuum, but not from the aspects considered in this report. Most of the particles of this interplanetary gas have been fully ionized into the plasma state of matter. Of all the observable baryonic matter<sup>1</sup> in the universe, 99 % of it is estimated to be in the plasma state.[1] A plasma is a quasi-neutral ionized gas with free electrons and ions with their motion being mainly determined by electromagnetic forces, and differ from regular gases in which collisions between individual particles dominate the particle motion. Of course collisions may occur in a plasma as well as electromagnetic forces could affect the motion of particles in a regular gas, but the dominating forces on a particle in a plasma is the electromagnetic forces.

The fact that electromagnetic forces dominates results in a rather complicated dynamic behaviour of plasmas, at the level of individual particles. For instance let us take a brief look at an electron in a plasma. It moves under the influence of an electromagnetic field, produced by every other electric particle and any external background field. This motion in turn gives rise to a change in the electromagnetic field influencing all other particles and changing the forces acting upon them and so on. This means that the complexity of motion of plasma particles quickly grows beyond what is possible to manage and one is forced to simplify the problem of motion by looking at the *collective behaviour* of several plasma particles together. One major benefit with true plasmas, as compared to regular gases, is that such an approach is indeed possible. As long as there is a large number of particles in a Debye sphere, i.e. a sphere of volume  $\frac{4\pi}{3}\lambda_D^3$ , where the Debye length  $\lambda_D$  is defined in equation 1.1, collective effects will dominate the dynamics, making it possible to work with averages and densities rather than with individual particle motion.

---

<sup>1</sup>Baryonic matter consists of three quarks, for example the two lightest baryonic particles are the proton and the neutron.

## 1.2 Plasma parameters

One parameter which determines the behaviour of plasma particles is the density, or more specifically the number density, which in this report it will be given in terms of number of particles per unit volume. Due to the quasi-neutrality of plasma the density for electrons, denoted by  $n_e$ , is approximately equal to the density of ions, denoted by  $n_i$ , as long as the ions are positive and singly charged. This number of particles per unit volume will in the following text, if not otherwise explicitly expressed, simply be denoted  $n$  as  $n \approx n_e \approx n_i$ .

One other parameter which determines the behaviour of plasma particles is the temperature, which is often different between the lighter electrons and the heavier ions. In this report, we assume that the temperature of the ions,  $T_i$ , equal to that of the electrons,  $T_e$ , as the ions are less important for our purpose. If there is a magnetic field present in the plasma the temperature of both electrons and ions could even be different parallel and perpendicular to this field. This situation has not been modelled in this report, as it is not yet implemented in the simulation software used<sup>2</sup>, and adds much complexity to the simulations.

One major plasma parameter describing the collective behaviour of the plasma particles is the Debye length, denoted by  $\lambda_D$  and defined as

$$\lambda_D \equiv \sqrt{\frac{\epsilon_0 K T_e}{n_e e^2}}, \quad (1.1)$$

where  $\epsilon_0$  is the permittivity in free space,  $K$  is Boltzmann's constant and  $e$  is the electron charge. The Debye length is a measurement of the shielding effect the plasma exerts on a potential. A simple qualitative example of when shielding occurs is if for instance a collector (such as a Langmuir probe, see section 3.1) is inserted into a quasi-neutral plasma and this collector is given a positive potential relative to the plasma. The negatively charged electrons will be attracted by this potential and begin to move closer to it. As the local density of electrons increases around the positive collector they cancel the effect of the potential and decrease the potential further away from the collector. At a certain distance the potential will be almost completely cancelled out and the Debye length is a measurement of this effect, which is called Debye shielding.

This means that for our assumption of quasi-neutrality to be valid we must consider a plasma which extends over distances larger than the Debye length.

---

<sup>2</sup>The software used for this report was SPIS version 3.7 RC09, see section 4.1 for a brief description of the software or Appendix A for a brief guide on how to use the software.

## Chapter 2

# Cassini-Huygens Spacecraft

### 2.1 Introduction

The Cassini-Huygens spacecraft, on a joint mission between NASA, ESA and the Italian space agency, Agenzia Spaziale Italiana (ASI), was launched on the 15th of October 1997 and reached its orbit around the outer giant planet Saturn on July 1, 2004, after fly-bys of Venus, Earth and Jupiter. Previous spacecraft that have visited Saturn include Pioneer 11 (in 1979), Voyager 1 (1980) and Voyager 2 (1981), all of which were fly-by missions. One of the main objectives of Cassini is not to investigate the planet Saturn itself but in fact one of its larger moons, Titan. A major reason for this is that Titan has an atmosphere consisting of several different complex molecular species, with similarities to that of Earth in its infancy. Cassini has since it reached its orbit around Saturn been able to investigate this in detail and the upper atmosphere of Titan has indeed been found to consist of several more or less complex molecules.[2]

### 2.2 The Cassini orbiter

The main body of the Cassini spacecraft resembles a cylinder in shape with a length of 5.09 meter and a varying radius from 0.9 meter to 1.125 meter. On top of one of the end sides there is a high gain antenna, 4 meters in diameter, making the total length of the Cassini spacecraft approximately 6 meters and one of the largest interplanetary spacecrafts ever constructed. Onto the sides of the main body there are some 12 different instruments and cameras mounted, and prior to its release the Huygens probe resided on the side of the Cassini spacecraft. The Huygens probe was released down through the atmosphere of Saturn's largest moon Titan during one of the spacecraft's fly-bys and carried six different instruments to measure the properties of Titan. This release, interpreted by an artist, is shown in figure 2.1. One striking feature on the side of the Cassini spacecraft is the 11 meter long boom for the magnetometer. Another of the instruments, mounted on the side of the Cassini spacecraft, is the Langmuir probe belonging to the Radio and Plasma Wave Science group, see section 3.1.



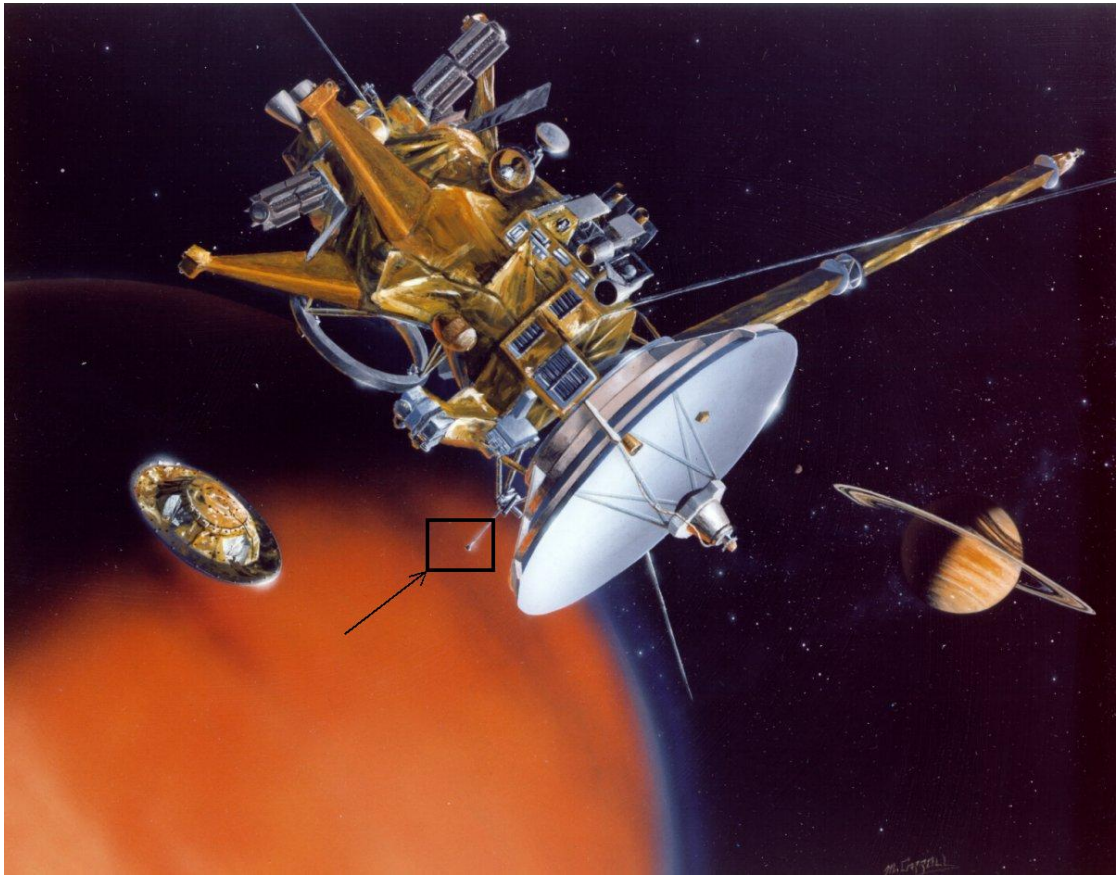


**Figure 2.1:** Artists interpretation of the Huygens probe separating from the Cassini spacecraft. The position of the Langmuir probe is shown by the black arrow and box. Courtesy NASA/JPL-Caltech. ID number: ESASBDUTYWC

## Chapter 3

# The Langmuir probe

### 3.1 The instrument

One of the instruments on board the Cassini spacecraft, see section 2.1, is the Langmuir probe, LP, which is designed to measure the plasma surrounding Saturn and its moons. The LP has been designed by the Swedish Institute of Space Physics Uppsala division (IRF-U) as a part of the Radio and Plasma Wave Science group (RPWS). The Langmuir probe consists of a sphere with 50 mm diameter and stub with a diameter of 6.35 mm and a length of 10.9 cm attached to this sphere.[3] The sphere and the stub are both made out of titanium with a titanium nitride coating and both are held at the same potential relative to the plasma by the connected electronics. A boom of length 0.8 meter with a diameter of 9.53 mm (at the interface with the stub) attaches the LP to the magnetic coil assembly and thereby to the rest of the spacecraft. This boom is held at the same potential as the rest of the spacecraft. The boom and stub gives a total distance of 1.5 m between the LP and the main body of the Cassini spacecraft. The LP and its boom is shown in its undeployed state in figure 3.1, and the mounting on the spacecraft is seen in figure 2.1. The Langmuir probe works by measuring the current flowing from the sphere to the surrounding plasma, and by varying the potential of the probe a so called potential sweep can be obtained. The Langmuir probe has the capability of making potential sweeps where the potential is changed in 256 steps from -32 V to +32 V in less than 1 s.[4] From these potential sweeps various plasma parameters can be determined using the theoretical model described in section 3.2.

### 3.2 Probe theory

When working with current collection by a body in a plasma, the laws of motion for individual particles quickly grows beyond what is comfortable and manageable, and therefore two different sets of approximations are convenient to use depending on the plasma one is interested in studying. One is called Sheath limited regime, in which the radius of the collector,  $r$ , satisfies  $r \gg \lambda_D$ . The other approach is the Orbit motion limited, OML-theory, in which  $r \ll \lambda_D$ , [5], which is of much interest to us.

A spherical Langmuir probe can in most cases be considered a perfect sphere, and as such there exist a theoretical model for the current between the probe and the surrounding plasma.

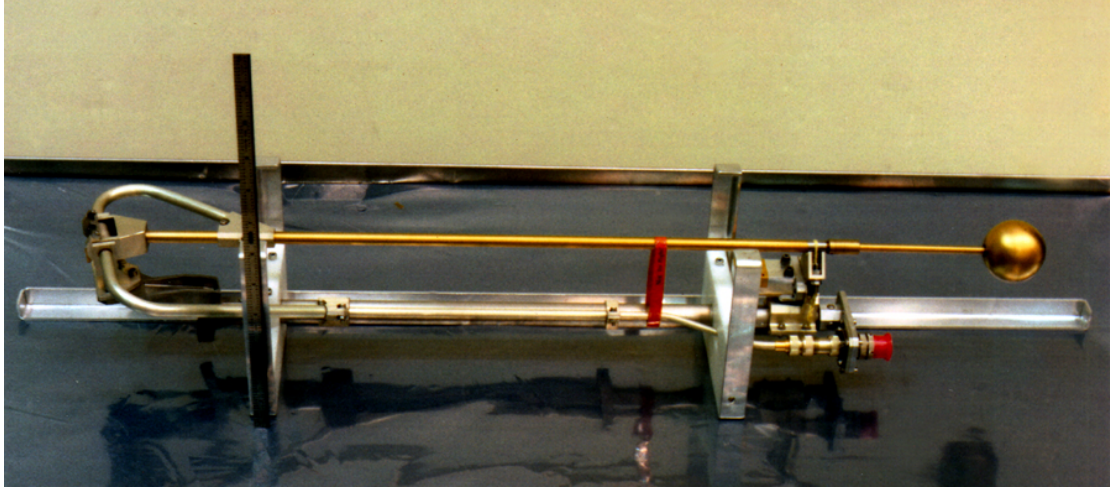


**Figure 3.1:** *The Langmuir probe and its boom in its undeployed state.*

The theoretical expressions for the current given here assume that we have a plasma under the OML-theory, that its distribution is Maxwellian, and that it consist of single charged ions (only hydrogen is used in this report).

If  $V$  is the voltage of the probe with respect to the plasma, we have for  $V < 0$  that

$$I_e = I_{e0} \exp\left(\frac{eV}{KT_e}\right) \quad (3.1)$$

$$I_i = -I_{i0} \left(1 - \frac{eV}{KT_i}\right), \quad KT_i \gg \frac{1}{2}m_i v^2 \quad (3.2)$$

where  $I_e$  is the electron current and  $I_i$  the ion current.  $T_e$  and  $T_i$  corresponds to the temperature of the electrons and ions respectively.  $K$  is Boltzmann's constant and  $e$  is the electron charge.

In the cases simulated in this report there is no ram current as the plasma and probe is considered stationary with respect to each other,  $\vec{v} \approx \vec{0}$ , the plasma particles only have their thermal and accelerated motion due to the potential of the probe.

For  $V > 0$ :

$$I_e = I_{e0} \left(1 + \frac{eV}{KT_e}\right) \quad (3.3)$$

$$I_i = -I_{i0} \exp\left(-\frac{eV}{KT_i}\right) \quad (3.4)$$

where the random current is given by

$$I_{e0} = 4\pi r^2 n e \sqrt{\frac{KT_e}{2\pi m_e}} \quad (3.5)$$

$$I_{i0} = 4\pi r^2 n e \sqrt{\frac{KT_i}{2\pi m_i}} \quad (3.6)$$

where  $m_e$  and  $m_i$  corresponds to the electron and ion mass respectively.

This is however only an OML-theory approximation,  $r \ll \lambda_D$ , which is valid in the first simulation with the Langmuir probe described in section 6.2. However there will always be some sheath present preventing some particles from reaching the probe, especially when the probe radius is comparable to the Debye length which is the case in the second simulation with the Langmuir probe in section 6.3. And in this case some model for the sheath is required. The collected electron current will in this case, assuming spherical and concentric sheath, [6], instead be given by

$$I_e = I_{e0} \left(\frac{a}{r}\right)^2 \left(1 - \frac{a^2 - r^2}{a^2} \exp\left(-\frac{r^2 eV}{KT_e (a^2 - r^2)}\right)\right) \quad (3.7)$$

where the sheath radius,  $a$ , is complicated to derive but has been modelled by Walker, [7], as

$$a = r + 0.83\lambda_D \sqrt{\frac{V}{KT_e}} \sqrt[3]{\frac{r}{\lambda_D}}. \quad (3.8)$$

For the ion current however the case is much more complicated, and the theoretical model used for comparisons to simulation in this report is the model developed by Kanal,[8] , as cited by Whipple.[6]. This ion current is given below in equation 3.9

$$I_i = \frac{\pi r^2}{2} n_i e v \left\{ \left[1 + \frac{\alpha^2}{2v^2} - \left(\frac{U}{v}\right)^2\right] \left[erf\left(\frac{v+U}{\alpha}\right) + erf\left(\frac{v-U}{\alpha}\right)\right] + \frac{\alpha}{\sqrt{\pi v}} \left[ \left(\frac{U}{v} + 1\right) \exp\left(-\left(\frac{v-U}{\alpha}\right)^2\right) - \left(\frac{U}{v} - 1\right) \exp\left(-\left(\frac{v+U}{\alpha}\right)^2\right) \right] \right\} \quad (3.9)$$

where

$$\alpha = \sqrt{\frac{2kT_i}{m_i}} \quad (3.10)$$

$$U = \sqrt{\frac{2eV}{m_i}} \quad (3.11)$$

$$erf(x) = \frac{2}{\sqrt{\pi}} \int_0^x \exp(-u^2) du \quad (3.12)$$

It should be noted that this ion current is valid for all repulsive potentials and for attractive potentials only<sup>1</sup> as long as  $r\sqrt{1 - \frac{2eV}{m_i V^2}} < a$ .

As the instrument only measures the total net current we have

$$I(V) = I_e + I_i. \quad (3.13)$$

For the Langmuir probe instrument on board the Cassini spacecraft, see section 2.1, the total current also include a photoemission current when the probe is in sunlight. In addition, the

---

<sup>1</sup>Therefore there may be some deviations in the negative part of the sweep between the theoretical and simulated Langmuir probe described in section 6.3.

current is influenced by the stub and spacecraft itself. The influence of the stub and the fact that the Langmuir probe is not a perfect sphere surrounded by plasma is investigated in this report, and the results for the probe can be found in chapter 6 while the influence of the spacecraft is presented in chapter 5. The influence of the photoelectron current is not investigated in this report but the model of the Langmuir probe, included in Appendix B.2, could easily be modified to allow for future simulations to investigate to what extent the photoelectrons influence the measurements made by the Langmuir probe, with the stub partly shaded or fully sunlit.

## Chapter 4

# Spacecraft plasma interaction system, (SPIS)

### 4.1 Introduction

The spacecraft plasma interaction system, SPIS<sup>1</sup>, has been developed by ONERA/DESP, Artenum and University Paris VII through an ESA contract<sup>2</sup> and is released under an open-source license. The program aims to simulate the effects of plasma on spacecrafts, although it can be and has been used to simulate all sorts of various plasmas and their interactions with conductive or isolating materials in solid state, not only spacecrafts. The main code is written in Java and comes packaged together with several third part programs, also released under open licenses, utilized by SPIS to, for instance, model and mesh the spacecraft and volume of plasma to be simulated. The SPIS code models the plasma particles not at the level of individual electrons and ions, which would require to much computational power, but instead as macroparticles in a so called particle-in-cell (PIC) approach.[9] The PIC approach is commonly used for plasma simulation codes. Each macroparticle is equivalent to a number of physical plasma particles. This number is indirectly defined by the user input, and these macroparticles are then moved around in the simulation volume accordingly. In order to perform simulations of the Cassini spacecraft and the Langmuir probe in various space plasma some simplifications of the spacecraft model are required.

### 4.2 Model of Cassini

The main body is modelled as a cylinder of varying radius and a length of 5.09 meter. The Huygens probe is omitted, as it was released into the atmosphere of Saturn's moon Titan during one of Cassini's early fly-bys and it would therefore not affect most of the measurements made by the Langmuir probe. The high gain antenna is modelled as a parabolic disc with a small gap between it and the main body of Cassini. The SPIS software however considers the two parts as one electric node and they are therefore given the same potential. The magnetometer boom is modelled with quadratic cross-section and approximately 90 degrees from this, the boom attaching the LP, see section 3.1, is situated. This boom was modelled as a simple cylinder of constant radius and connected directly to the Cassini spacecraft. However, due to the large difference in size between the LP and the spacecraft, the probe and stub was omitted in this

---

<sup>1</sup>The SPIS software can be downloaded from <http://dev.spis.org/projects/spine/home/spis/>.

<sup>2</sup>ESA contract Nbr: 16806/02/NL/JA.

model and simulations on them run separately. In the model, the boom attaching the LP to the Cassini spacecraft is surrounded by an outer virtual cylinder in order for the 3D meshing to go from a very fine mesh around the position where the LP would be, if it were modelled, to a coarser mesh on the spacecraft itself. The Cassini spacecraft is then in turn surrounded by a couple of boxes increasing in size to the boundary at least two  $\lambda_D$  away from any part of the spacecraft for the same reason. This model is shown in figure 4.1 where the magnetometer boom and the boom attaching the LP is clearly visible. The model used in the simulations in this report is given in the appendix B.1.

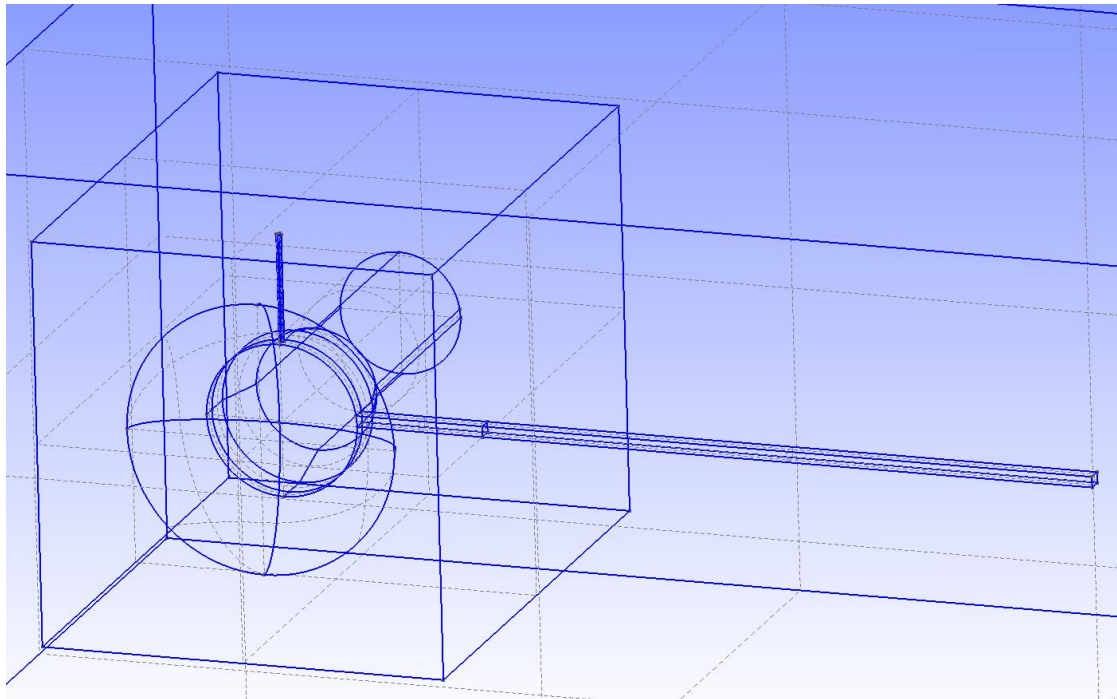


**Figure 4.1:** *The model of the Cassini spacecraft with the magnetometer boom and the boom attaching the LP to the spacecraft, used for this report.*

### 4.3 Model of the Langmuir probe

The Langmuir probe, see section 3.1, is also simplified in order to carry out the simulations. The Langmuir probe was modelled as a sphere, with radius 2.5 cm, with the stub attached. The stub is properly modelled as a 10.9 cm long cylinder with a radius of 3.175 mm mounted on the Langmuir probe sphere, while the boom connecting the stub to the Cassini spacecraft was omitted. Keeping the boom would drastically increase the complexity of the simulations as the simulation box would need to increase drastically in size and the boom should be kept at the same potential as the Cassini spacecraft would have had in the same plasma. To compensate

for this simplification, the end of the stub was given an individual physical id and was kept at zero potential relative to the plasma to minimize its effect. The Langmuir probe model is then surrounded by increasingly bigger cylinders in order to allow for the 3D meshing to go from a very fine mesh on the probe itself to a bit coarser mesh on the boundary. The probe together with the two innermost cylinders is shown in figure 4.2, while the model file is given in the appendix B.2.

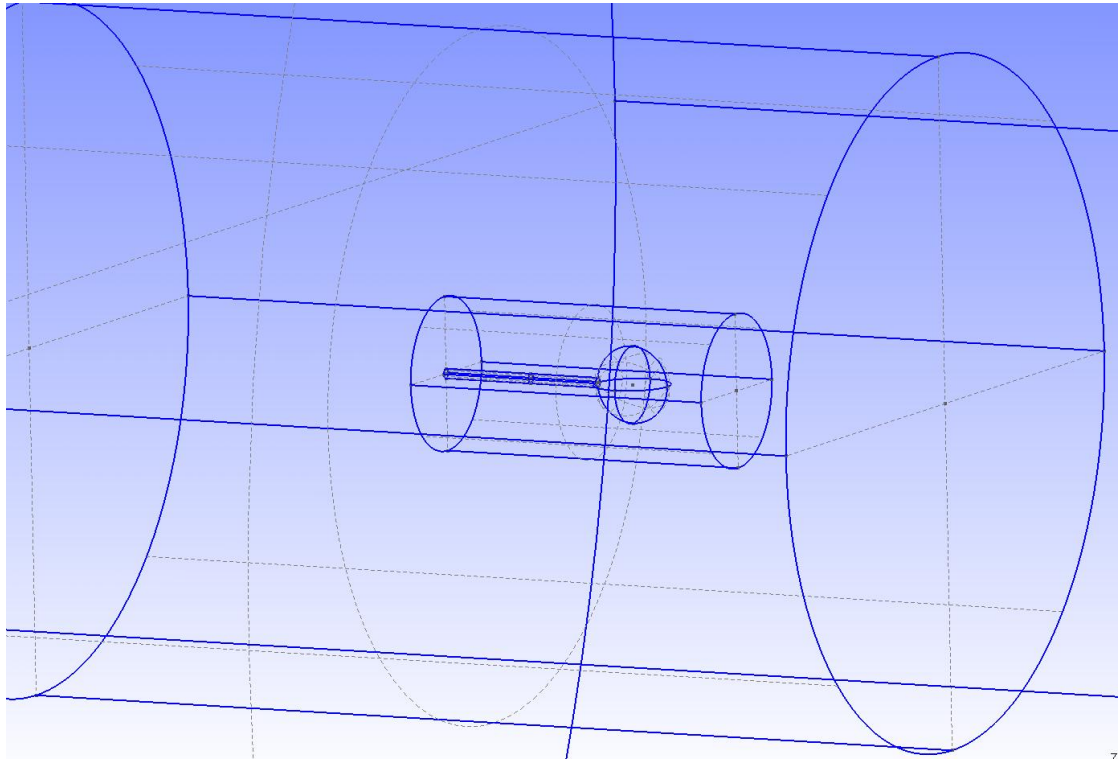


**Figure 4.2:** *The model of the Langmuir probe with its stub, used for this report.*



# Chapter 5

## Results of Cassini simulations

### 5.1 Introduction

Due to the spacecraft potential, the potential in the plasma outside the spacecraft, will decay due to Coulomb's law, further assisted by Debye shielding, which is shortly described in section 1.1. However, when dealing with plasmas with longer Debye length the potential will still correspond to a significant fraction of the temperature of the particles, in the short distance from the boom on the spacecraft to the collecting sphere of the Langmuir probe. Therefore this remaining potential will influence the plasma particles with an increased (or decreased) potential as compared to if only the Langmuir probe was charged with a potential. How much this extra potential will be is investigated in this chapter by simulating the Cassini spacecraft, see section 2.1, in various plasmas.

The Cassini spacecraft was simulated in several plasmas with varying Debye length, from the shortest Debye length of 0.235 meter for a plasma with  $n_e = 100$  per cubic centimetre and  $T_e = 0.1$  eV to the longest Debye length of 74.3 meter in a plasma with  $n_e = 0.01$  per cubic centimetre and  $T_e = 1$  eV. For a complete list of the different temperatures and densities used see appendix C. During each of these simulations the size of the simulation box boundary was adopted to be at least two  $\lambda_D$  away from any part of the spacecraft. During each simulation the spacecraft potential was allowed to be floating, beginning at zero, and to stabilize at a value<sup>1</sup>, where the net current is essentially zero, before the ratio of the remaining spacecraft potential at the position of the Langmuir probe was calculated.<sup>2</sup> Please note that due to the large difference in size between the probe and the spacecraft, the probe and stub had to be omitted in these simulations and run separately, and the results of the LP simulations are given in chapter 6.

In order to simulate the plasma with the shortest and longest Debye lengths, modelling of the electron population was switched from the PIC approach, used in all other simulations in this report, to a simple Maxwellian distribution governed by the local potential in each mesh cell, in turn governed by the local density of ion macroparticles. The Maxwellian distribution approach is permissible in this case since in this dense plasma, the spacecraft potential should be negative and the Maxwell-Boltzmann distribution retains its shape in a repulsive potential. This approach could be used in this type of simulation, whereas in the simulation done of the

---

<sup>1</sup>The spacecraft stabilizes, as expected when the net current in equation 3.13 is zero, at a potential of approximately  $-2.5 \times T_e$ .

<sup>2</sup>The plasma potential was measured in the point [5.01; 0; 2.625] (for the coordinate system used in appendix B.1) and this was compared to the potential of the spacecraft itself.

LP, described in chapter 6, this would not work as in that case one is interested in the current (of actual macroparticles) to or from the probe.

## 5.2 Results

As shown in figure 5.1 the plasma potential, at the position of the probe, drops down to essentially zero for very short Debye lengths. This is just as expected, since a short Debye length means that we have a strong Debye shielding effect. For longer Debye lengths on the other hand it is evident that the remaining potential stabilizes at around 0.76, meaning that the plasma potential has decreased to 76 % of the spacecraft potential.

For example, let's take a plasma with electron temperature 1 eV and Debye length 70 m. In this plasma, the spacecraft would reach a stable potential of about -2.5 V. According to the simulation results shown in figure 5.1 the potential would decrease to 76 %, meaning that -1.9 V would still remain at the position of the Langmuir probe and influence the current measured.

For this case, with the long Debye lengths this means that the probe only measures a 24 % drop in potential, the so called probe-to-spacecraft potential  $V_{ps}$ . And this in turn means that the actual potential of the spacecraft,  $V_{sc}$  can be calculated as  $V_{sc} = \frac{V_{ps}}{0.24} \approx 4.16V_{ps}$ . This is close to the value derived from measurements made by other instrumentation onboard, in which this value is somewhere in the region of 5 to 6.[10]

In figure 5.2 the decreasing plasma potential around the Cassini spacecraft is visualized in a plane containing the boom attaching the Langmuir probe to the spacecraft for a plasma with density of one per cubic centimetre and a temperature of one electron volt. The non-zero potential at the probe position is obvious. And figure 5.3 shows the same plane but for a plasma with shorter Debye length, this plasma had a density of 100 per cubic centimetre and a temperature of 0.1 electron volt.

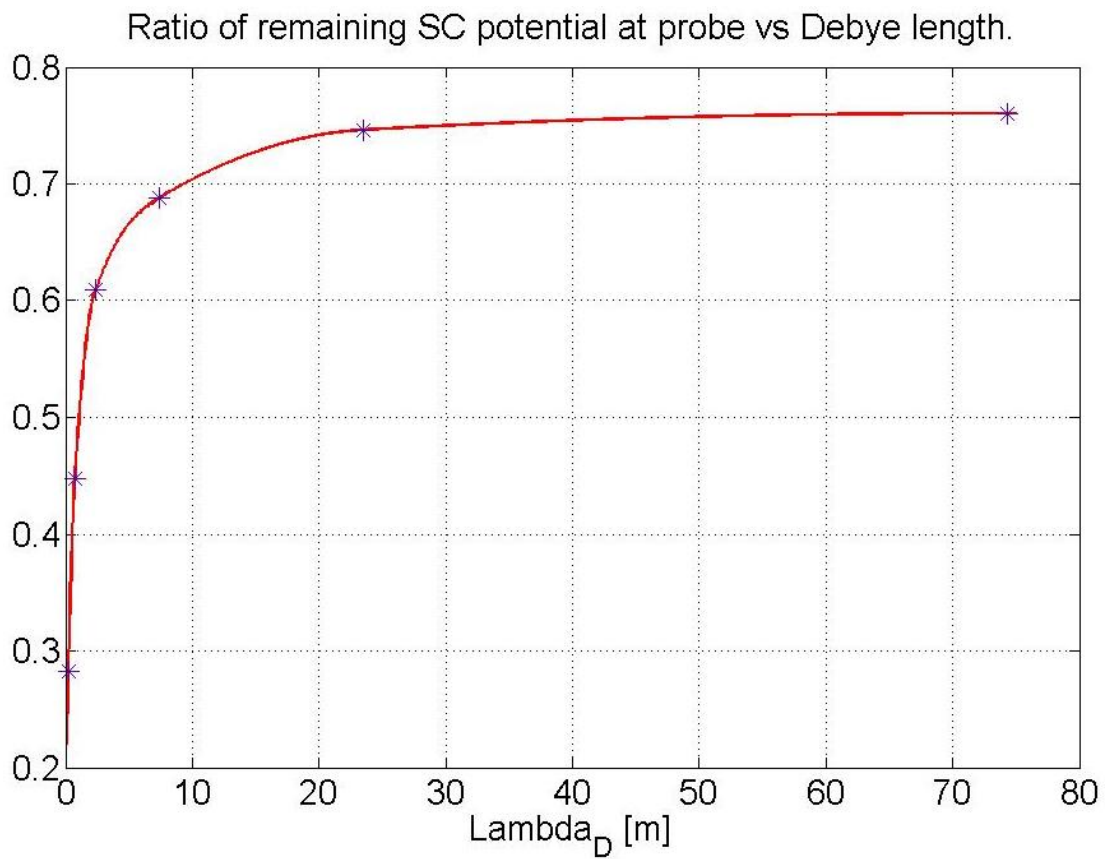


**Figure 5.1:** Ratio of remaining spacecraft potential at the probe distance from Cassini for plasmas with varying Debye lengths.

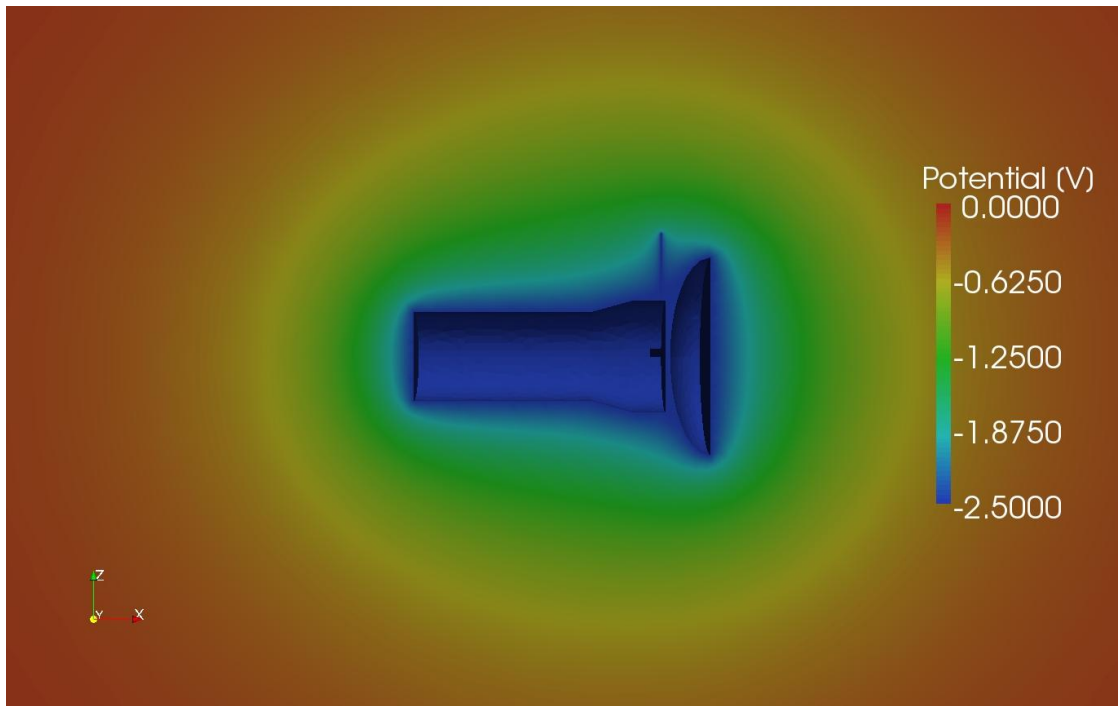


**Figure 5.2:** Showing the Cassini spacecraft and the surrounding plasma potential in a plane along the boom attaching the LP to the spacecraft, for a plasma with density 1 per cubic cm and temperature 1 eV.

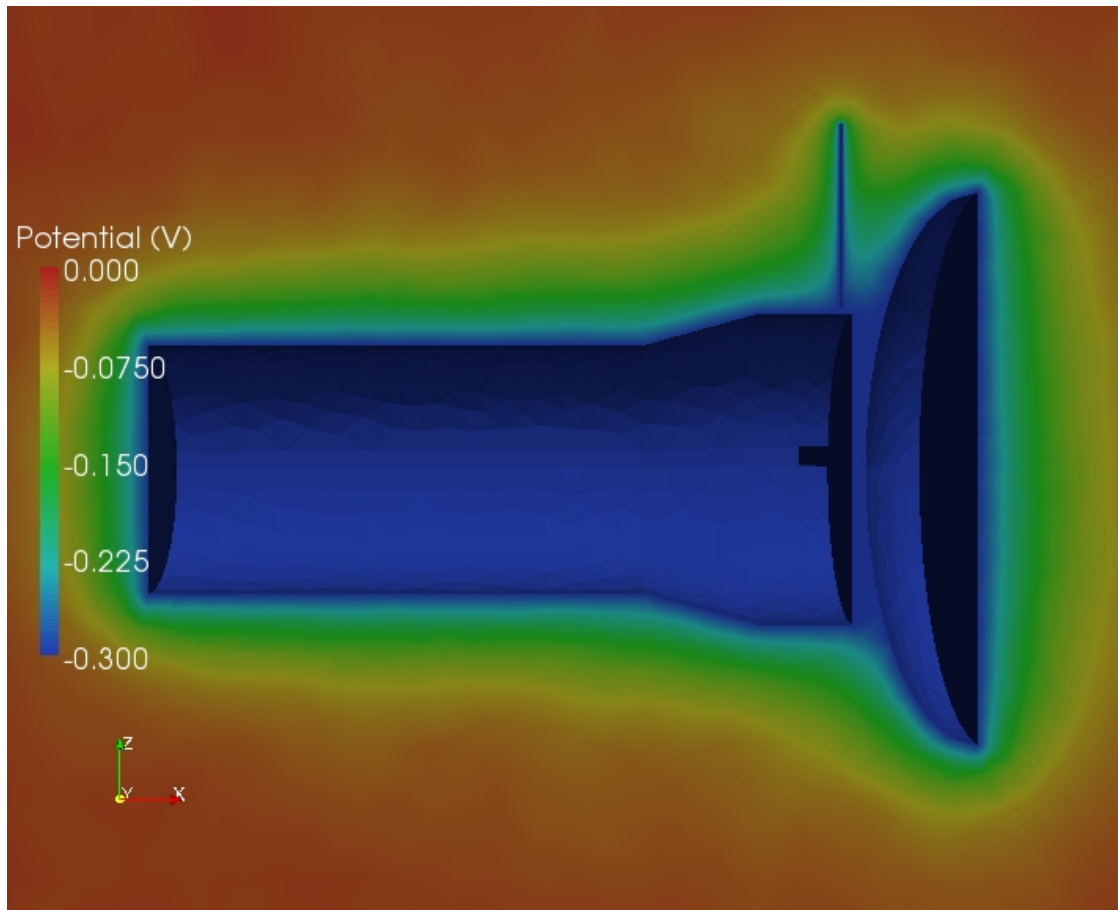


**Figure 5.3:** Showing the Cassini spacecraft and the surrounding plasma potential in a plane along the boom attaching the LP to the spacecraft, for a plasma with density 100 per cubic cm and temperature 0.1 eV.

# Chapter 6

## Results of Langmuir probe simulations

### 6.1 Introduction

Here the results of two different simulation cases for the Langmuir probe are presented, in the first case a low density plasma with a Debye length, given by equation 1.1, much larger than the size of the Langmuir probe, see chapter 3.1, is used. In the second case the plasma has a density and temperature appropriate to the ionosphere of Titan: the density is 1,000 times that of the first case, so the Debye length in this case is approximately of the same size as the diameter of our probe. Remember that OML-theory can be considered a good approximation as long as the probe radius is (much) less than the Debye length. In both cases the Langmuir probe is simulated with its stub and a regular sphere without the stub is also simulated for control purposes and only the current to the spherical probe is measured.

### 6.2 Low density $1 \text{ cm}^{-3}$ and high temperature 1 eV

In this simulation the density was set to one particle per cubic centimetre and the temperature was set to one eV. This gives a Debye length of 7.43 meters which is much larger than the dimensions of the Langmuir probe, thereby ensuring that OML-theory as described in section 3.2 is a valid approach for the theoretical modelling of probe current collection. It is interesting to note that the current collected for the simulated sphere, shown in figure 6.1, agrees with the theoretical value almost perfectly, while the derivative, shown in figure 6.2, shows some minor numerical deviations. This gives us reason to believe that these simulations are reliable. On the other hand the simulated sweep for the Langmuir probe together with the stub shows a small deviation in the total collected current, slightly lower current is collected than what is expected for a perfect sphere, and in the derivative there is slightly more noise than there is in the simulations with only a sphere. This deviation between the simulated perfect sphere and the Langmuir probe with the stub present is approximately 4 %.

When comparing the control, the simulated sphere, to the current predicted by OML-theory it is found that the relative deviation varies from -2.5 % to +1.0 % for the positive potential, as shown in figure 6.3. The deviation being calculated as the relative difference in simulated current compared to the current predicted by OML for each potential that was simulated, i.e.  $[I_{\text{sphere}}(V) - I_{\text{OML}}(V)] / I_{\text{OML}}(V)$ . Previous work done in validating the SPIS software has in some cases shown a deviation between the simulated results and OML-theory of approximately 5 %.[11]

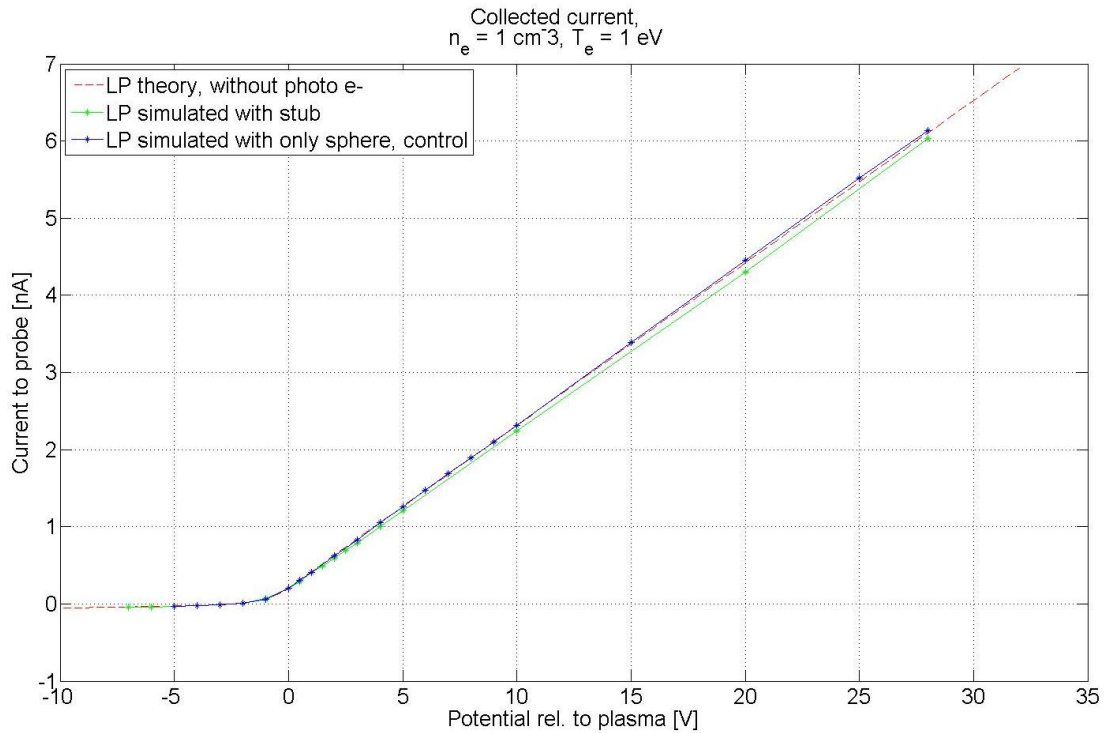


**Figure 6.1:** Collected current for a Langmuir probe without any photoelectrons in a plasma with density 1 per cubic cm and temperature 1 eV. The red dashed line corresponds to the theoretical current for a perfect sphere, blue line marked with stars represent the simulated current for a perfect sphere and the green line marked with stars is the current for the simulated Langmuir probe with the stub present but not including the current to it.

According to OML-theory the probe current,  $I_p$  is proportional to the surface area,  $A_p$ . Laframboise has even shown that this should be true even if the collector is ellipsoidal in shape, as long as the assumption for OML-theory is valid.[12]. This means that for the Langmuir probe, with the stub present, we could expect a decrease in probe current due to the interface of the stub itself. But this would only account for approximately 1 % decrease in current.

Note that the current flowing to the stub is not included and that each star in the diagrams represents one simulation, typical CPU time for each simulation was about three hours.

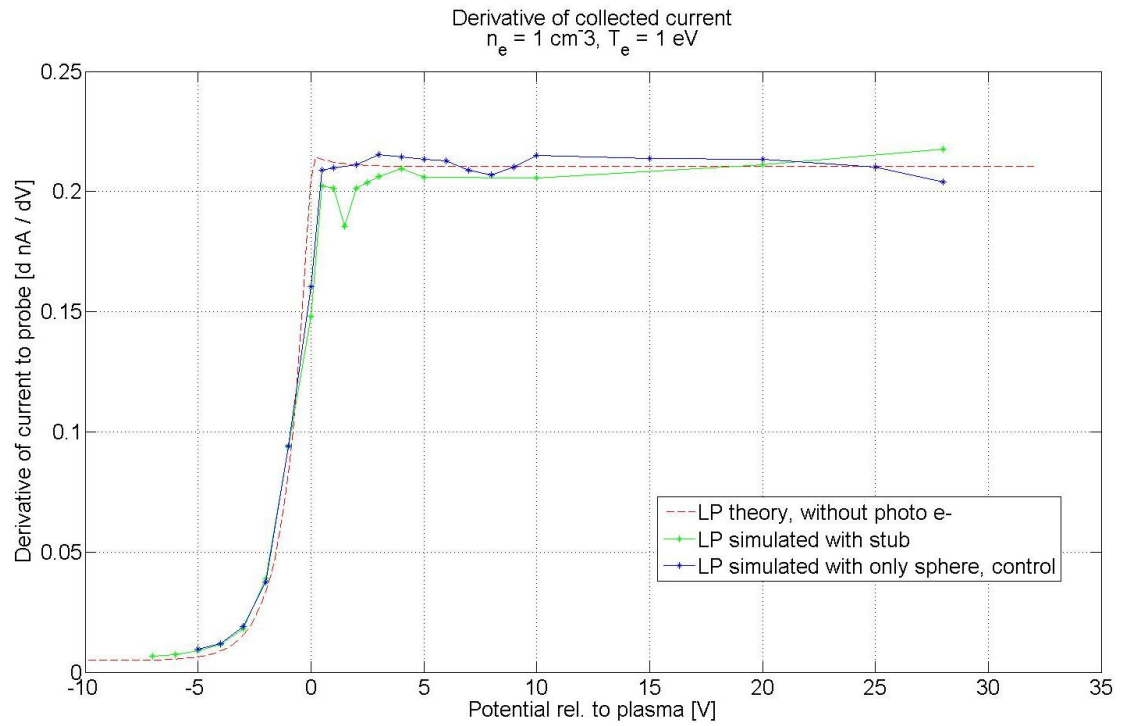


**Figure 6.2:** Derivative of the collected current for a Langmuir probe without any photoelectrons in a plasma with density 1 per cubic cm and temperature 1 eV. The red dashed line corresponds to the theoretical derivative the of current collected for a perfect sphere, blue line marked with stars represent the simulated case for a perfect sphere and the green line marked with stars corresponds to the derivative of the current for the simulated Langmuir probe.



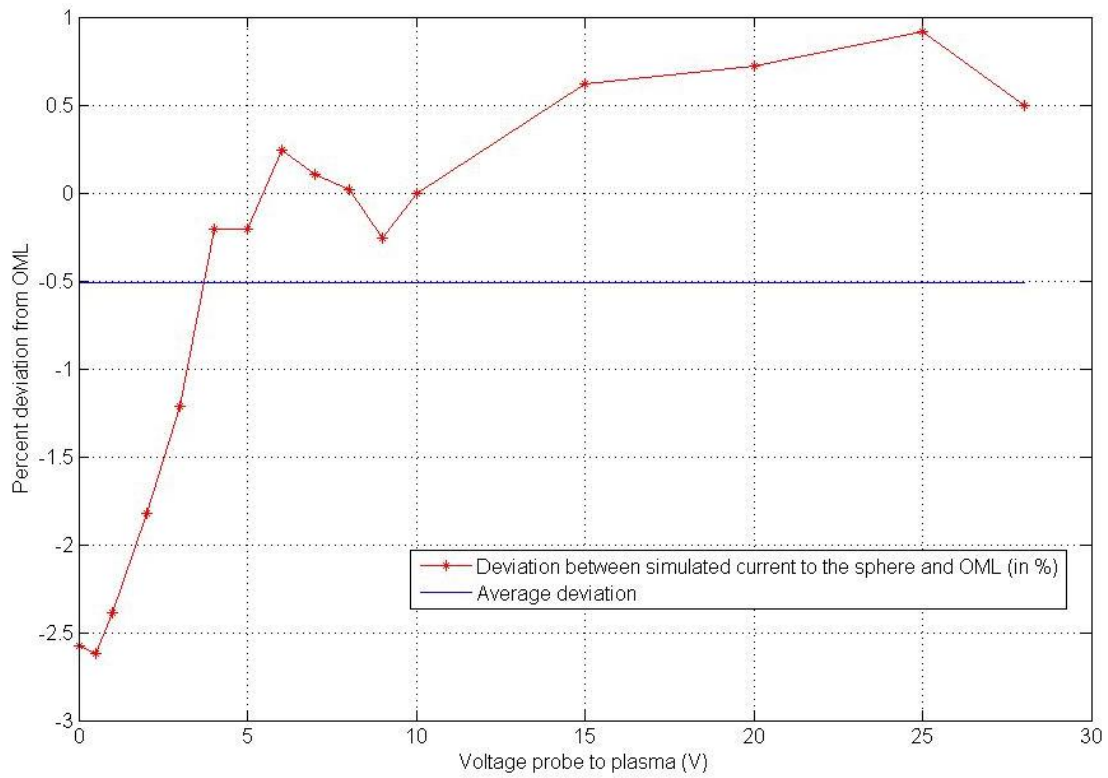


**Figure 6.3:** Deviation between the collected current for the sphere and the current predicted by OML-theory. In a plasma without any photoelectrons and a density of 1 per cubic cm and temperature 1 eV. The red line with stars corresponds to the deviation for each positive potential simulated and the blue line corresponds to the average deviation.

### 6.3 High density $1,000 \text{ cm}^{-3}$ and low temperature $0.05 \text{ eV}$

In the second case the density is increased to 1,000 particles per cubic centimetre and the temperature is lowered to 0.05 eV, which is comparable to the plasma in the ionosphere around Saturn's moon Titan.[13] As a result of the lower temperature, 0.05 eV, the total sweep was reduced in size to  $\pm 1 \text{ V}$  as compared with the low density case in section 6.2. This was made in order to ensure that the plasma potential would be able to drop below the temperature of the different particles being injected at the boundary. Once again a perfect sphere, without the stub present, is simulated to ensure that the simulations are carried out in a correct fashion. The collected current is shown in figure 6.4, and this current lies above the predicted values for a theoretical sphere according to Walker.[7] See section 3.2 for a description of this theoretical curve. However there seems to be more agreement with the predicted curve that comes from the work made by Laframboise.[14] On the other hand, when looking at the simulations of the Langmuir probe with the stub present the current collected is lower than the current collected to the simulated perfect sphere, the same situation as for the lower density case described in section 6.2, the only difference is that the deviation is bigger. But for some reason the current in this case, with shorter Debye length, is slightly higher than the theoretical value predicted by Walker for an ideal sphere. The reason for omitting Laframboise curve in the low density case is that there is no distinct difference between the Laframboise, Walker or OML curves when OML-theory is applicable.

The area of used for current collection, in the case of the Langmuir probe together with its stub, is smaller due to the stub interface itself. However, this could be easily be corrected by simply reducing the size of the perfect sphere one uses to compare against. The Langmuir probe sphere has a radius of 2.5 cm, the reduction in area would correspond to a perfect sphere of radius 2.495 cm and this do not explain the deviation shown in figure 6.4, the change in current collected due to the changed radius is almost negligible. And the deviation between the simulated Langmuir probe, with stub, and the theoretical value predicted by the Walker sheath model would only increase with this correction of probe area.

When looking at the derivative of the collected current for this case, shown in figure 6.5, one needs to bear in mind that there are fewer simulations done in this case as compared with the low density case, thereby the jagged look of the curve. And it's even more clear that there is a bigger difference between the simulations made with and without the stub present, than in the case with longer Debye length. The deviations in this case is about 7 to 8 percent, as compared with 3 to 4 percent in the case with longer Debye length.

In figure 6.6 the decreasing plasma potential around the Langmuir probe with its stub is visualized in a plane alongside the stub, when the LP is held at a potential of +1 V.

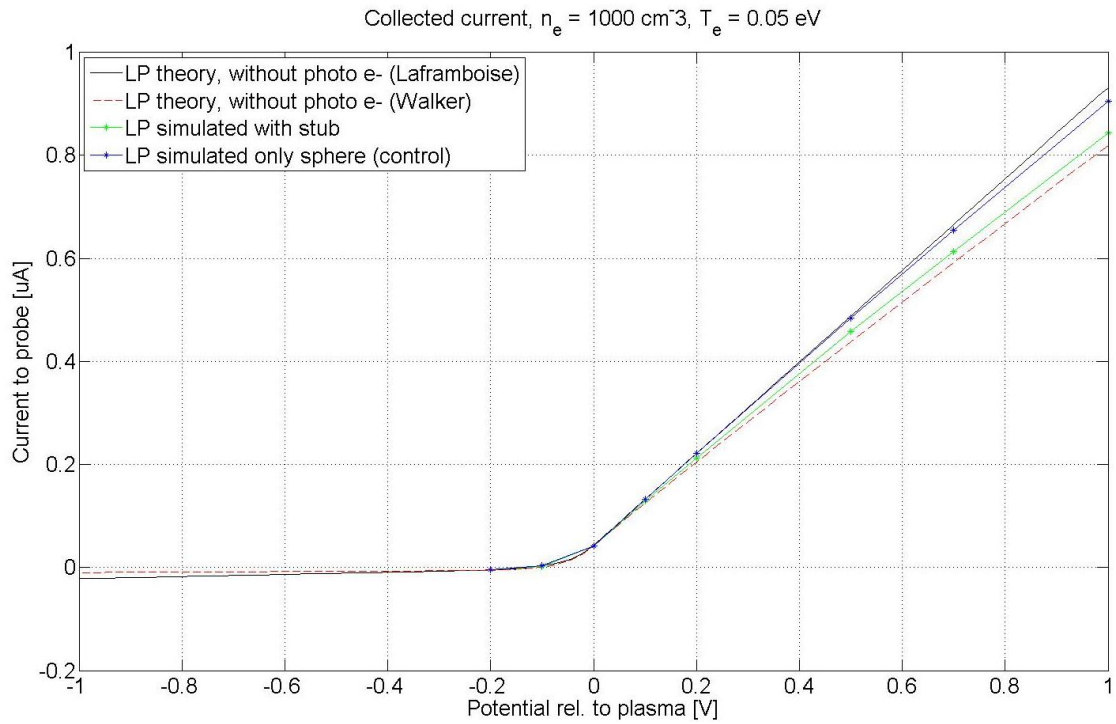


**Figure 6.4:** Collected current for a Langmuir probe without any photoelectrons in a plasma with density 1,000 per cubic cm and temperature 0.05 eV. The red dashed line corresponds to the theoretical current for a perfect sphere (Walker theory same as in the low density case), the black line represents the theoretical curve based on Laframboise, blue line marked with stars represent the simulated current for a perfect sphere and the green line marked with stars is the current for the simulated Langmuir probe. Please note that the theoretical ion current for the attractive potential is not yet validated and therefore no direct results can be drawn from the negative part of this sweep, see section 3.2, and only a few simulations are done with negative potential.

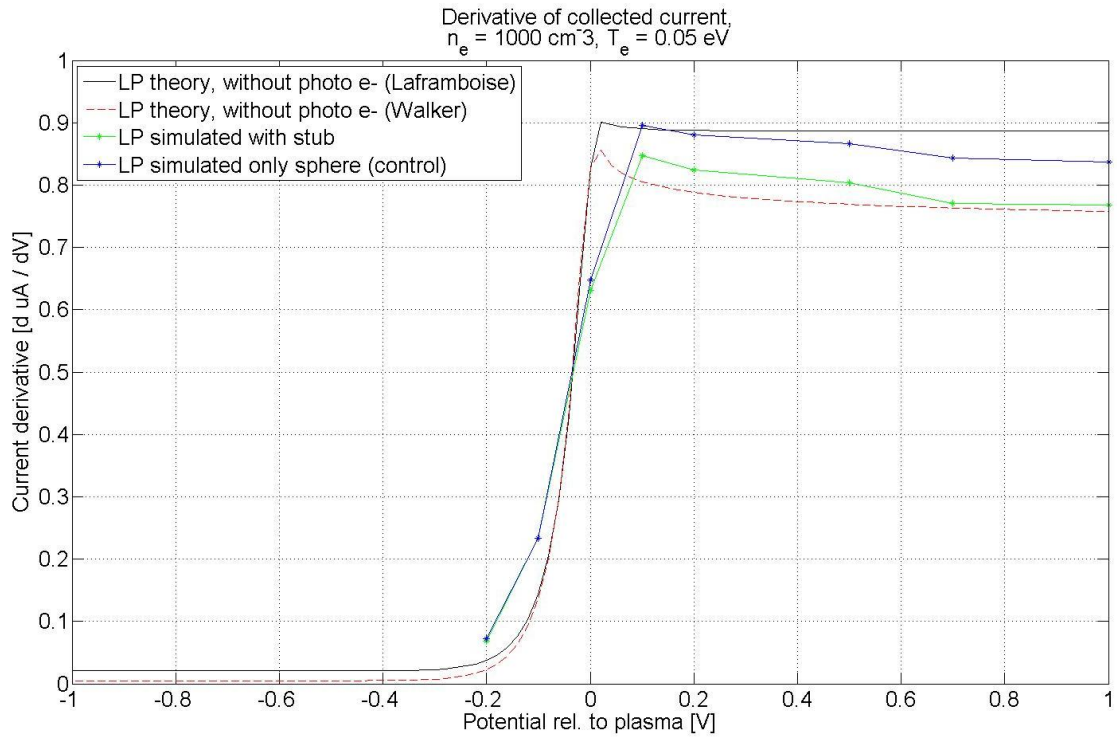


**Figure 6.5:** Derivative of the collected current for a Langmuir probe without any photoelectrons in a plasma with density 1,000 per cubic cm and temperature 0.05 eV. The red dashed line corresponds to the theoretical derivative of the current collected for a perfect sphere (Walker theory), the black line corresponds to the theoretical curve based on Laframboise, the blue line marked with stars represent the simulated derivative of current for a perfect sphere and the green line marked with stars corresponds to the derivative of the current for the simulated Langmuir probe. Please note that the theoretical ion current for the attractive potential is not yet validated and therefore no direct results can be drawn from the negative part of this sweep.

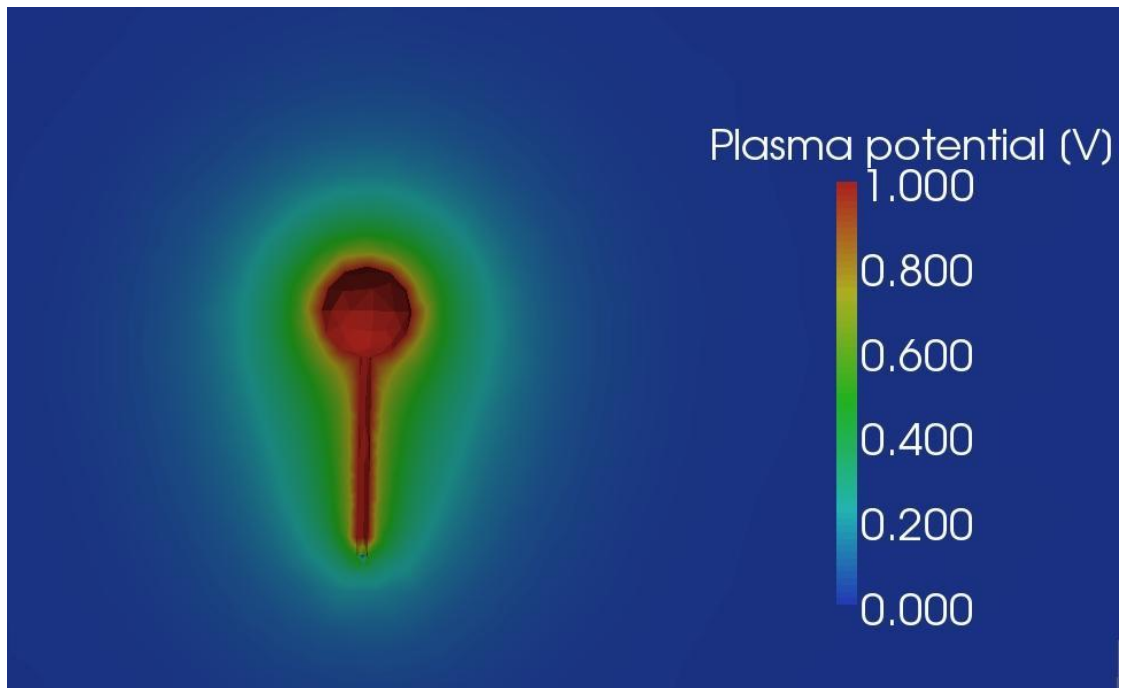


**Figure 6.6:** *Plasma potential surrounding the Langmuir probe with the stub, both having the fixed potential +1 V relative to plasma at infinity. The plasma density is 1,000 per cubic cm and temperature 0.05 eV*

# Chapter 7

## Conclusions and outlook

### 7.1 Conclusions

The presence of the Cassini spacecraft will, for a plasma without photoelectrons, decrease the potential of the plasma at the position of the probe, as compared with what the potential would be if the spacecraft was not present. For a plasma with long Debye length the potential of the plasma will decrease to 76 % of the spacecraft potential at the position of the probe. This means that to calculate the spacecraft potential from the probe-to-spacecraft potential, measured by the LP, a factor of 4.16 will have to be used. This value is slightly lower than the empirical value used up to this point.

When considering the presence of the stub and its effect on the current collected to the probe there seems to be only a minor difference when dealing with a plasma with long Debye length, for which OML-theory would be valid. The only difference is that the current the probe collects,  $I_p$ , is slightly less (approximately 4 %) then it would be for a perfect sphere. This should be held in comparison with the 1 % decrease in probe area due to the interface of the stub and this seems reasonable.

For a plasma with shorter Debye lengths on the other hand the deviation in the probe current,  $I_p$ , with and without the stub increases to approximately 7 %. And the Walker model seems to need some further adaptations if it's to be used for analysis of Langmuir probe measurements.

### 7.2 Outlook

A couple of things have been omitted in this report and could possibly be examined in the future. Among which is the affect photoelectrons may have on the measurements. The model of the Langmuir probe, with and without stub present, used for this work could with ease<sup>1</sup> be adopted to examine how different angles towards the sun could affect the current flowing to and from the sphere. (I.e. if a bigger portion of the stub is sunlit one could expect that more photoelectrons would be measured by the probe). The simulations of the Langmuir probe, described in chapter 6, should be possible to replicate with a lower noise level and shorter CPU time in the new version of SPIS<sup>2</sup> which has the capability of doing backtracking. To be able to investigate the Cassini spacecraft in sunlight and looking at different angles towards the sun

---

<sup>1</sup>Following the description given in appendix A.

<sup>2</sup>The latest release of SPIS is v.4.0RC01, the version used for this report was v.3.7RC09.

some major development of the SPIS software is needed as the version used for this report don't handle shadowing of different spacecraft parts in a satisfactory way.

It could also be interesting to investigate how different flowing plasmas would affect the measurements made by the probe. However this would almost certainly have to be performed without sunlight. As the Cassini spacecraft orbits Saturn, and constantly change its attitude, it will almost always have the plasma flow in one direction and the sun angle in another.

# Bibliography

- [1] F. Chen, *Introduction to Plasma Physics and Controlled Fusion*, vol. 1. Springer Science+ Business Media, LLC, second ed., 1984.
- [2] J. H. Waite, H. Niemann, R. V. Yelle, W. T. Kasprzak, T. E. Cravens, J. G. Luhmann, R. L. McNutt, W.-H. Ip, D. Gell, V. De La Haye, I. Müller-Wodarg, B. Magee, N. Borggren, S. Ledvina, G. Fletcher, E. Walter, R. Miller, S. Scherer, R. Thorpe, J. Xu, B. Block, and K. Arnett, “Ion Neutral Mass Spectrometer Results from the First Flyby of Titan,” *Science*, vol. 308, pp. 982–986, May 2005.
- [3] D. A. Gurnett, W. S. Kurth, D. L. Kirchner, G. B. Hospodarsky, T. F. Averkamp, P. Zarka, A. Lecacheux, R. Manning, A. Roux, P. Canu, N. Cornilleau-Wehrin, P. Galopeau, A. Meyer, R. Boström, G. Gustafsson, J.-E. Wahlund, L. Åhlén, H. O. Rucker, H. P. Ladreiter, W. Macher, L. J. C. Woolliscroft, H. Alleyne, M. L. Kaiser, M. D. Desch, W. M. Farrell, C. C. Harvey, P. Louarn, P. J. Kellogg, K. Goetz, and A. Pedersen, “The Cassini Radio and Plasma Wave Investigation,” *Space Science Reviews*, vol. 114, pp. 395–463, Sept. 2004.
- [4] J.-E. Wahlund, R. Boström, G. Gustafsson, D. A. Gurnett, W. S. Kurth, T. Averkamp, G. B. Hospodarsky, A. M. Persoon, P. Canu, A. Pedersen, M. D. Desch, A. I. Eriksson, R. Gill, M. W. Morooka, and M. André, “The inner magnetosphere of Saturn: Cassini RPWS cold plasma results from the first encounter,” *Geophysical Research Letters*, vol. 32, pp. 20–+, Sept. 2005.
- [5] H. M. Mott-Smith and I. Langmuir, “The Theory of Collectors in Gaseous Discharges,” *Physical Review*, vol. 28, pp. 727–763, Oct. 1926.
- [6] E. C. J. Whipple, *The Equilibrium Electric Potential of a Body in the Upper Atmosphere and in Interplanetary Space*. PhD thesis, The George Washington University., 1965.
- [7] E. H. Walker, *Plasma Sheath and Screening around a Stationary Charged Sphere and a Rapidly Moving Charged Body*. PhD thesis, University of Maryland College Park., 1964.
- [8] M. Kanal, “Theory of Current Collection of Moving Spherical Probes.,” *Sci. Rept. No. JS-5, Space Physics Research Lab., Univ. of Mich.*, 1962.
- [9] J.-F. Roussel, F. Rogier, G. Dufour, J.-C. Mateo-Velez, J. Forest, A. Hilgers, D. Rodgers, L. Girard, and D. Payan, “SPIS Open-Source Code: Methods, Capabilities, Achievements, and Prospects,” *IEEE Transactions on Plasma Science*, vol. 36, pp. 2360–2368, Oct. 2008.
- [10] J.-E. Wahlund et al., “Detection of dusty plasma near the E-ring of Saturn,” *Planet. Space Sci.*, 2009. (in press).



- [11] A. Hilgers, S. Clucas, B. Thiebault, J. Roussel, J. Mateo-Velez, J. Forest, and D. Rodgers, "Modeling of Plasma Probe Interactions With a PIC Code Using an Unstructured Mesh," *IEEE Transactions on Plasma Science*, vol. 36, pp. 2319–2323, Oct. 2008.
- [12] J. G. Laframboise and L. W. Parker, "Probe design for orbit-limited current collection," *Physics of Fluids*, vol. 16, pp. 629–636, May 1973.
- [13] K. Ågren, J.-E. Wahlund, R. Modolo, D. Lummerzheim, M. Galand, I. Müller-Wodarg, P. Canu, W. S. Kurth, T. E. Cravens, R. V. Yelle, J. J. H. Waite, A. J. Coates, G. R. Lewis, D. T. Young, C. Bertucci, and M. K. Dougherty, "On magnetospheric electron impact ionisation and dynamics in Titan's ram-side and polar ionosphere - a Cassini case study," *Annales Geophysicae*, vol. 25, pp. 2359–2369, Nov. 2007.
- [14] J. G. Laframboise, "Theory of spherical and cylindrical Langmuir probes in a collisionless, Maxwellian plasma at rest," Tech. Rep. UTIAS report 100, Institute for Aerospace Studies, University of Toronto, 1966.
- [15] E. Kawamura, C. K. Birdsall, and V. Vahedi, "Physical and numerical methods of speeding up particle codes and paralleling as applied to RF discharges," *Plasma Sources Science Technology*, vol. 9, pp. 413–428, Aug. 2000.

# Appendix A

## Appendix: Simulations with SPIS

Here in this appendix a brief guide on how to setup and use SPIS will be given. The software SPIS itself is briefly described in section 4.1.

### A.1 Prior to beginning the simulations

There is likely a couple of different things you may need to update or change once you have downloaded and unpacked the SPIS program. In the version of SPIS used for this report<sup>1</sup> several third part programs included in the package are outdated and an update will have to be performed.

One of the third part programs requiring an update is called Gmsh, which handles the construction of the models and the 3D meshing of the plasma volume to be simulated in SPIS. For convenience I will here explain how to update SPIS to use the latest version of Gmsh, but of course the approach is identical for updating all of the third part programs included and used by SPIS. This will be explained for a Linux system, however it can easily be adopted to other systems as well.

1. Download the latest version of Gmsh from its official homepage<sup>2</sup> and extract it into the folder  
SPIS\_home/Thirdpart/Gmsh/Linux-I386/gmsh-2.3.0  
For a Windows system you would simply substitute *Linux-I386* for *Windows*.
2. Now you need to tell SPIS to use this unpacked version of Gmsh instead of the version included in the SPIS package. To do that simply open the configuration file  
SPIS\_home/SpisUI/Bin/config.py in your preferred text editor. Then change the appropriate line, in this case  
GL\_CMD\_GMSH = r"..ThirdPart/Gmsh/Linux-I386/gmsh-2.0.8/gmsh" to  
GL\_CMD\_GMSH = r"..ThirdPart/Gmsh/Linux-I386/gmsh-2.3.0/gmsh".
3. SPIS should now be ready to use the latest version of Gmsh, but in order to optimize the meshing performed by Gmsh you need to start Gmsh and activate one setting inside the program itself. This setting is called "optimize quality of tetrahedra" and it is found under

---

<sup>1</sup>The version of SPIS used for this report was 3.7RC09.

<sup>2</sup>Gmsh official homepage is <http://geuz.org/gmsh/> and the version used for this report was 2.3.0.

Tools - Options - Mesh - Advanced. After this change is done, you need to save this setting as the default setting, this is done by File - Save default option.

In some cases it could be required to use more memory in the SPIS simulations than the default value. In order to change this, increase the parameter *-Xmx1611m* in the file `SPIS_home/ThirdPart/Jython/jython-2.1/jython`.

## A.2 Building the model

The construction of models to be simulated is done in the third part program called Gmsh and in that program the user builds up the model point by point, connecting points to lines, lines to surfaces and then surfaces to volumes. This is a somewhat tedious work, and one needs to make sure each point is exactly where it should be in order for the lines to be connected properly. Any incorrectly placed points (or defined lines, surfaces, volumes) will not necessarily be reported to the user at this stage. SPIS will react to this error in a later stage without providing any useful error message and therefore it's important to make sure each previous step is correctly finished. One way of controlling that the model is correct is to use the visibility option under the Tools menu and control that each volume is correctly defined.

Once the model is constructed it is necessary to make sure the 3D meshing<sup>3</sup> works satisfactory. The fourth parameter in the .geo-file created by Gmsh controls the local size of each mesh at that point. This fourth parameter is called the characteristic length and is, in the same way as all the other coordinates, given in meters. If one, for instance, has a large volume of plasma with a smaller spacecraft that one wishes to simulate one could increase the mesh size on the boundary and keep it smaller at the spacecraft. But doing this too drastically could instead create long and narrow tetrahedrons in the volume in between, which is bad for the simulation. To eliminate this problem an intermediate volume could be created with a characteristic length somewhere in between the boundaries and the spacecraft's characteristic lengths. One requirement that determines the size of the tetrahedrons one can use is the Courant condition,[15] which leads us to use a largest characteristic length of approximately half the Debye length for PIC simulations.

## A.3 Running SPIS

Once your model is constructed, and you have made a mesh you think is sufficient but not too fine (otherwise the simulations will take forever) it is time to move into the program SPIS itself. To do that we use the user interface. The starting script is found in the folder `SPIS_home/SpisUI/` and you simply choose what is appropriate for your system. I have been using the one named `runSpisVTK5.sh`. Don't be alarmed if you where to receive an error message saying, 'Error in JavaLib: Impossible to load vtkParallelJava', this error message can be ignored. The user interface is built up in several steps one need to go through, symbolized by icons on the second row, and they are called in the order they are listed from left to right. Ignoring the first two,

---

<sup>3</sup>Gmsh meshes the volume into tetrahedrons by default but this could be changed into cubic form which could work better for some models.

which corresponds to saving and loading previous project, the first one to be used is the *'Call the CAD tools'*.

**'Call the CAD tools'**: Here one need to add the file (or files) containing the model one wishes to use. Do this by clicking the 'Add' button and select your file.<sup>4</sup> Once you have added your file(s) you must define one main file. Do this by selecting your file in the list and click on 'Set as main'. This must be done even if you only have one file. Thereafter you could close this window by clicking on the 'x', but this is the only window previous to running your simulation that you should close in this way.

After that you can continue with *'Load geom'* and *'Property'*, to load the geometry and the default properties for different materials. In the next step, *'Call the GEOM-property groups editor'*, the different physical parts of the simulation is given their respective properties. The different physical parts are defined in the .geo-file.

**'Call the GEOM-property groups editor'**: Here the program lists all your different physical parts as defined in the .geo-file and the program itself adds three groups with the description Default points/surfaces/volumes. These can be deleted as they no longer have any meaning.<sup>5</sup> The different groups corresponding to different physical parts **must** be ordered in the following way: first the outer boundary (of the type surface), secondly the spacecraft (also of the type surface) and last but not least the volume containing the plasma (of type volume). For this reason I have named my physical ID increasingly for the different types and each of the physical groups should by default have the settings described in table A.1.

Physical	Material	ElecNode	Plasma
Boundary	None	None	Boundary, default
Spacecraft	ITO, default	Spacecraft ground (ElecNode-0)	Spacecraft, default
Plasma	None	None	Plasma Model in Volume, default

**Table A.1:** *Default settings for the physical groups in the order they should be listed.*

Of course one could change the material of the spacecraft group to some other material, which closer resembles the material of the real spacecraft, and one could also split the spacecraft group into several different parts and give each a different electrical node. This could be useful if one is interested in the current collected to only one part of the spacecraft as in the Langmuir probe simulations where only the current to the sphere is of interest, however one part must be defined as spacecraft ground and all other nodes must be defined in the file called by *'electricCircuitFilename'*. (see the *'Call the Global parameters editor'* below).

When all of this is done you click 'ok'.

Thereafter you continue with *'Call the mesher'*, *'Convert the GEOM (CAD) groups into mesh groups'* and *'Map (deploy) the fields on the mesh according to groups'*. When you have made sure your model is correct you can later omit these three steps and simply continue to *'Call*

<sup>4</sup>The file should be in .geo format. For an example of a working model feel free to try my model of Cassini given in the appendix B.1, also available at [http://space.irfu.se/exjobb/2009\\_thomas\\_nilsson/](http://space.irfu.se/exjobb/2009_thomas_nilsson/).

<sup>5</sup>They where required by previous version of SPIS without being added automatically giving a lot of problem for users but the code has since changed and this has for some reason been left behind.

*the Global Parameter editor*'. These steps will be done automatically in the following steps if omitted.

**'Call the Global Parameter editor'**: Here most of the different settings for each simulation are made. Most of the settings will here be omitted and it's left to the user to make sure all settings necessary for the user's need have been set properly.<sup>6</sup> The settings are ordered into different groups, 'Volume interactions' (no changes necessary), 'B Field' (SPIS can at the moment not handle magnetic fields, no changes necessary), 'Simulation control' (some changes made, see headline lower in this document), 'Plasma' (some changes made, see headline lower in this document), 'Output' (no changes necessary), 'Poisson equation' (some changes made, see headline lower in this document), 'Surface Interactions' (some changes made, see headline lower in this document) and 'Spacecraft' (some changes made, see headline lower in this document).

**'Simulation control'** Under this group it could be required to change the default time each simulations should continue running until. This time have to be set by taking into account: box sizes, flow and thermal speeds, etc.

**'Plasma'** Under this group the user defines the plasma parameters to be used in the simulation. 'AvPartNbPerCell' defines the average number of macroparticles SPIS should place in each tetrahedron in the beginning of the simulation. The average number of particles per cell multiplied by the number of tetrahedrons divided by 1.5 approximately gives the total number of macroparticles. 'electronDensity' is the electron density of the first population electrons, given in per cubic meter. This differs from the most used convention which is per cubic centimetre, see section 1.2. 'electronDistrib' is the distribution class for the first population of electrons, the default value is 'PICVolDistrib' which means that they are modelled as macroparticles but this could be changed to 'GlobalMaxwellBoltzmannVolDistrib' in case one is not interested in simulating their motion and one can assume a perfect Maxwellian distribution. This was done for some simulations of Cassini, see section 4.2 with very short Debye length, given in equation 1.1. 'electronSpeedUp' is used to reduce the motion of the electron particles, normally the electrons move several times faster than the ions and this means that SPIS has to keep moving the electrons around a lot compared with the ion particles, due to their difference in mass. To reduce CPU time this setting is used to simply move the electron macroparticles a fraction of that time, but one should be very careful when using this setting to make sure it is used properly. Given equal temperature it could be set as high as the square root of the mass ratio between the ions and electrons. 'electronTemperature' is the temperature for the first population electrons, given in eV.

In a similar way, 'ionDensity' and 'ionTemperature' are defined. 'ionVx', 'ionVy' and 'ionVz' is the incoming velocity of the ion particles as they enter the simulation box with the Cartesian coordinate system being the same as Gmsh used when the model was constructed. The velocity is given in meters per second and just as any other parameter it could be set using scientific notation, i.e. 1.0E2 for 100 and so on.

**'Poisson equation'** Here, among other things, the user defines which requirements of accuracy SPIS should use. One other parameter the user can set is which type of Poisson solver

---

<sup>6</sup>The user should also make sure that the settings are in fact used by the code itself and not only in the user interface. For an updated list of settings and their usage please see the file SPIS\_home/Doc/DocSpisNum/HowTo/Controlling NUM from UI.html.

should be used, linear or non-linear. This setting only has effect when using a Maxwell distribution for the electron population.

'*Surface Interactions*' Here one can change how the program will handle particles hitting the spacecraft, if for instance second emission particles should be used or whether photoelectrons should be included. The current version of SPIS has some difficulties handling photoelectrons in a satisfactory way<sup>7</sup> and therefore some different approaches may be adopted in order to solve some of the different problems that may occur. It could be activated by changing the setting 'photoEmission' to 1, 3, 5 or 7. When using the value 1 or 5 SPIS simply allows the current to flow from the surface without regarding the photoelectrons as particles once they have left the surface, 1 being the global approach which takes input from sun direction and 5 being the locally defined flux (up to the user to make sure only parts facing the sun has the material setting for photo emission on). None of these two are of interest in this report. With 3 or 7 however the photoelectrons are treated as macroparticles in the same way as the electrons or ions. 3 meaning that the global setting is used taking input from the sun direction, i.e. taking care of curved parts of the spacecraft, and 7 meaning a locally defined flux.

When using a sun flux from the global setting, 'sunX', 'sunY' and 'sunZ' defines the direction towards the sun, but the user must note that if this vector has a length different from unit the flux will be scaled by this length. Unit length corresponds to having the sun at one astronomical unit.<sup>8</sup>

If one wishes to use the global approach and treat the photoelectrons as particles, 'photoEmission' is set to 3, and thereby taking input from the sun vector to make sure curved parts will emit the corresponding amount of photoelectrons. If one's spacecraft has different parts shaded and sunlit the user must make some small changes to the material properties as described below. To do this the user could use any Java editor/compiler, for instance eclipse.<sup>9</sup>

1. Open the files *Spis\_home/SpisNum/src/spis/Top/Default/SpisDefaultMaterials.java* and *Spis\_home/SpisNum/src/spis/Surf/SurfInteract/NascapParamSet.java*
2. Choose one material not used in your current model which you could overwrite with the material properties of the material used in your model.
3. You may want to change its name to know that it has changed, but this is not necessary as long as you yourself remember. Once you have overwritten one or more materials change the 13th parameter which corresponds to 'Photoelectron current for normally incident sunlight [A/m<sup>2</sup> at 1 AU]' of this material to zero. Thereby forcing the photo emission off.
4. Compile the code and replace the original file *Spis\_home/SpisNum/spis.jar* with your output file. But make sure you have a backup of the original file first, if anything has gone wrong or if you need to revert back to the original for your next simulations.

---

<sup>7</sup>For instance when using the locally defined sun flux all parts of the surface will emit photoelectrons regardless of their direction towards the sun and when using the global approach no regard is taken to shading of different spacecraft parts.

<sup>8</sup>For this report the Cassini spacecraft was simulated being at Saturn at 9.5 AU, meaning the sun vector had a length of  $(1/9.5)^2 \approx 0.011$ .

<sup>9</sup>Eclipse official homepage is <http://www.eclipse.org/>.

5. Make your model spacecraft with different physical surfaces, one for the parts in sunlight and one for the parts in shadow. Then choose appropriate material, with or without photo emissions for these physical surfaces.

'Spacecraft' Here the user set things like the spacecraft potential, 'initPot', and whether or not this should be fixed or floating, 'electricCircuitIntegrate'. By editing the file called by 'electricCircuitFilename' the user can also allow different part of the spacecraft to have different potential relative to the spacecraft ground. This requires that the spacecraft model has parts with different physical identities and that those are given different 'elecNode' (see above). One part is however required to be named 'Spacecraft ground (ElecNode-0)'. In the file called by 'electricCircuitFilename', by default 'circuit.txt' found in Spis\_home/SpisUI/DefaultValues/, the first parameter tells the program it is the voltage (V), second parameter and third parameter tells between which electric nodes it concerns and the last parameter tells the value, by default 0. When using different electric nodes all must be represented in this file and all voltages must be relative to ground. When using a floating potential for the Cassini spacecraft the spacecraft capacitance, 'CSat' had to be changed since the potential of Cassini did not reach a stable value during the simulation time. By reducing this value it reaches a stable value quicker but the noise level increases and vice versa.

Please note, when the user has changed a value one must hit 'enter' and fully leave the cell for the new value to be saved into the interface and when all changes needed is done the user should click 'save and quit'.

After this is done it is time to convert the user input, '*Convert data from UI to NUM data structure*', and begin the simulation, '*Launch the numerical kernel and perform the simulation*'. The user will then be notified when the simulation itself starts, after everything has been built and prepared, by a simple pop-up window. It would be advisable for any new user to switch between the '*Jython Log*' and '*Standard Log*' window to-and-fro while SPIS builds and prepares the simulation as it may, on occasion, run into some problems (while only notifying the user in one of these log windows). Do not wait in vain!

## A.4 Taking care of the results

Once the simulations are completed another pop-up window will appear, and once this is done I strongly recommend saving the project (even if you have already done so beforehand). The next step is to take care of the results, this is done by using the '*Call the DataFields manager for data analysis, extraction and conversion*' and from here all the different data collected during the simulation can be accessed. The data is sorted under five different categories namely '*Particle trajectory*', '*pre-processing*', '*Time dependent data*', '*Data on spacecraft*' and '*Data in volume*'.

To access the plasma potential, used in this report for example in figure 5.2, first go to '*Data in volume*' and select the '*Final plasma potential*' in the list. This data firstly require a small conversion to make it smooth, at the moment its stored as distinct points defined by the mesh. (See section A.2 above). The conversion can be made into four different data types, for a smooth one select the '*View on*' data type called '*Cell*' and press '*Export to VTK*'.

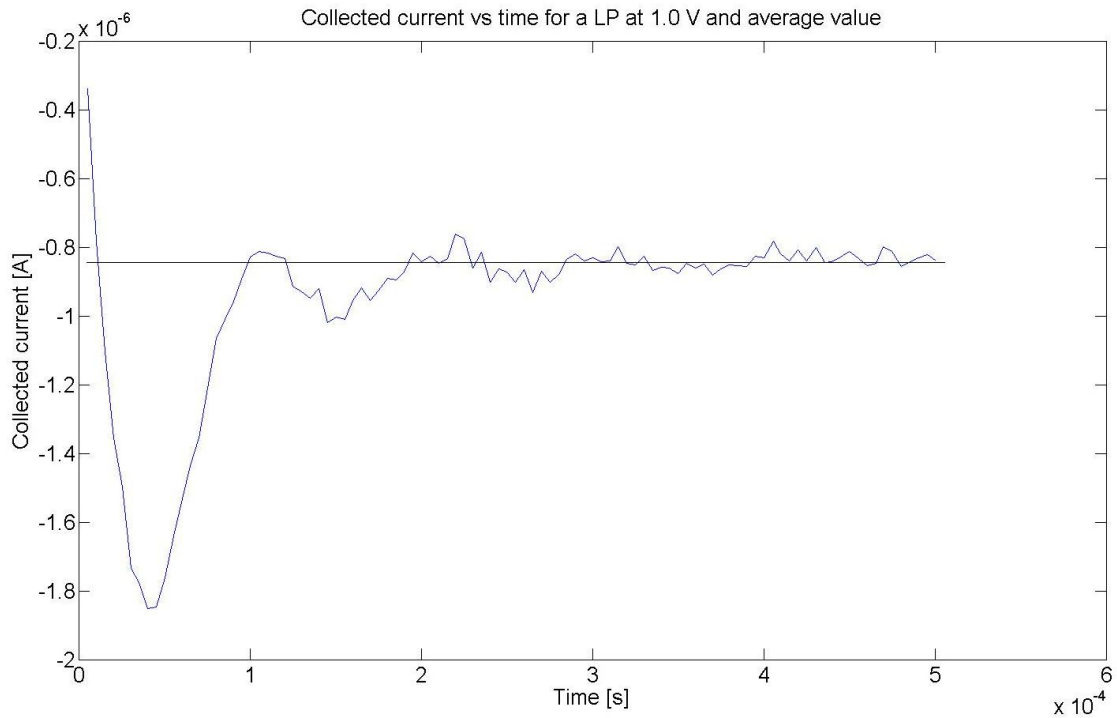


**Figure A.1:** Collected current for a Langmuir probe without any photoelectrons, at 1 V potential with respect to a plasma with density 1,000 per cubic cm and temperature 0.05 eV. The straight line corresponds to the average current, calculated using the latter half of the simulation. If one uses the entire simulation to calculate the current it will deviate from the theoretical predictions even for the simulations where OML is applicable.

Once this conversion has been completed, I recommend using Paraview<sup>10</sup> (included in the SPIS software package but not the default 3D viewer) for visualization of the now smooth 3D data.

One other thing accessible from this window is the collected current to each electrical node, defined by the user in table A.1, though when considering the current collected I have used the average value of the later half of this current data. This is because the simulation starts with an even spread of macroparticles all over the simulation volume and it therefore collects more current at the very first simulation steps. This is illustrated by figure A.1

<sup>10</sup>The latest version of Paraview and manuals for the software can be found on <http://www.paraview.org/>.



# Appendix B

## Appendix: Models used

### B.1 Cassini model

```
----- Cassini.geo -----
1 ////////////////////////////////////////////////////////////////////
2 // Copyright Thomas Nilsson //
3 ////////////////////////////////////////////////////////////////////
4 // Parameters for the mesh //
5 // and for size of simulation box //
6 ////////////////////////////////////////////////////////////////////
7
8 r_lp_bom=0.00953;
9 lambda=7.43;
10
11 cl_bom=0.5;
12 cl_out=lambda/3;
13 cl_int=0.8;
14 cl_inn=0.4;
15 cl_out_LP=0.03;
16 cl_in_LP=0.02;
17 cl_sc=0.20;
18
19
20 ////////////////////////////////////////////////////////////////////
21 // Intersection between //
22 // inner box and bom //
23 ////////////////////////////////////////////////////////////////////
24
25 Point(14001) = {4.865, 3, 0, cl_bom};
26 Point(14002) = {5.09, 3, 0, cl_bom};
27 Point(14003) = {4.865, 3, 0.1582113010464356, cl_bom};
28 Point(14004) = {5.09, 3, 0.1582113010464356, cl_bom};
29 Line(14005) = {14001, 14003};
30 Line(14006) = {14003, 14004};
31 Line(14007) = {14004, 14002};
32 Line(14008) = {14002, 14001};
33 Line Loop(14009) = {14006, 14007, 14008, 14005};
34 Plane Surface (14010)={14009};
35
36
37 ////////////////////////////////////////////////////////////////////
38 // Points for outer boundary //
39 // 2*Lambda_d away from any SC part //
40 ////////////////////////////////////////////////////////////////////
41
42 X=2;
43
44 Point(2009) = {-X*lambda, -2-X*lambda, -2-X*lambda, cl_out};
45 Point(2010) = {-X*lambda, -2-X*lambda, 2+X*lambda, cl_out};
46 Point(2011) = {-X*lambda, 12+X*lambda, 2+X*lambda, cl_out};
47 Point(2012) = {-X*lambda, 12+X*lambda, -2-X*lambda, cl_out};
48 Point(2013) = {6+X*lambda, 12+X*lambda, -2-X*lambda, cl_out};
49 Point(2014) = {6+X*lambda, 12+X*lambda, 2+X*lambda, cl_out};
50 Point(2015) = {6+X*lambda, -2-X*lambda, 2+X*lambda, cl_out};
51 Point(2016) = {6+X*lambda, -2-X*lambda, -2-X*lambda, cl_out};
52
53
54 ////////////////////////////////////////////////////////////////////
55 // Points for intermediate volume //
56 // (lambda/3) away from any SC part //
57 ////////////////////////////////////////////////////////////////////
58
59 Point(14005) = {6+lambda/3, 12+lambda/3, -2-lambda/3, cl_int};
60 Point(14006) = {-lambda/3, 12+lambda/3, -2-lambda/3, cl_int};
```

```

61 Point(14010) = {-lambda/3, 12+lambda/3, 2+lambda/3, cl_int};
62 Point(14014) = {6+lambda/3, 12+lambda/3, 2+lambda/3, cl_int};
63 Point(14026) = {-lambda/3, -2-lambda/3, 2+lambda/3, cl_int};
64 Point(14030) = {-lambda/3, -2-lambda/3, -2-lambda/3, cl_int};
65 Point(14038) = {6+lambda/3, -2-lambda/3, -2-lambda/3, cl_int};
66 Point(14042) = {6+lambda/3, -2-lambda/3, 2+lambda/3, cl_int};
67
68
69 ////////////////////////////////////////////////////
70 //          Points for inner volume          //
71 //          1 m away from most of SC          //
72 ////////////////////////////////////////////////////
73
74 Point(5007) = {7, 3, -3, cl_inn};
75 Point(5008) = {-1, 3, -3, cl_inn};
76 Point(5012) = {-1, 3, 3, cl_inn};
77 Point(5016) = {7, 3, 3, cl_inn};
78 Point(5028) = {-1, -3, -3, cl_inn};
79 Point(5032) = {7, -3, -3, cl_inn};
80 Point(5044) = {7, -3, 3, cl_inn};
81 Point(5048) = {-1, -3, 3, cl_inn};
82
83
84 ////////////////////////////////////////////////////
85 //          Points for volume around boom          //
86 ////////////////////////////////////////////////////
87
88 Point(7001) = {5.01, 0, 2.734, cl_out_LP};
89 Point(7002) = {5.01+4*r_lp_bom, 0, 2.734, cl_out_LP};
90 Point(7003) = {5.01, 4*r_lp_bom, 2.734, cl_out_LP};
91 Point(7004) = {5.01, -4*r_lp_bom, 2.734, cl_out_LP};
92 Point(7005) = {5.01-4*r_lp_bom, 0, 2.734, cl_out_LP};
93 Point(7006) = {5.01, -4*r_lp_bom, 1.15, 2*cl_out_LP};
94 Point(7007) = {5.01, 0, 1.15, 2*cl_out_LP};
95 Point(7008) = {5.01-4*r_lp_bom, 0, 1.15, 2*cl_out_LP};
96 Point(7009) = {5.01, 4*r_lp_bom, 1.15, 2*cl_out_LP};
97 Point(7010) = {5.01+4*r_lp_bom, 0, 1.15, 2*cl_out_LP};
98
99
100 ////////////////////////////////////////////////////
101 //          Points for the actual bom          //
102 ////////////////////////////////////////////////////
103
104 Point(7011) = {5.01-r_lp_bom, 0, 2.491, cl_in_LP};
105 Point(7012) = {5.01-r_lp_bom, 0, 1.18, 2*cl_in_LP};
106 Point(7016) = {5.01, 0, 1.18, 2*cl_in_LP};
107 Point(7017) = {5.01, r_lp_bom, 1.18, 2*cl_in_LP};
108 Point(7021) = {5.01, r_lp_bom, 2.491, cl_in_LP};
109 Point(7025) = {5.01, 0, 2.491, cl_in_LP};
110 Point(7029) = {5.01, -r_lp_bom, 1.18, 2*cl_in_LP};
111 Point(7041) = {5.01+r_lp_bom, 0, 1.18, 2*cl_in_LP};
112 Point(7050) = {5.01, -r_lp_bom, 2.491, cl_in_LP};
113 Point(7073) = {5.01+r_lp_bom, 0, 2.491, cl_in_LP};
114
115
116 ////////////////////////////////////////////////////
117 //          Circles and lines for volume          //
118 //          around bom          //
119 ////////////////////////////////////////////////////
120
121 Circle(7001) = {7005, 7001, 7003};
122 Circle(7002) = {7003, 7001, 7002};
123 Circle(7003) = {7002, 7001, 7004};
124 Circle(7004) = {7004, 7001, 7005};
125 Circle(7005) = {7006, 7007, 7008};
126 Circle(7006) = {7008, 7007, 7009};
127 Circle(7007) = {7009, 7007, 7010};
128 Circle(7008) = {7010, 7007, 7006};
129 Line(7009) = {7006, 7004};
130 Line(7010) = {7005, 7008};
131 Line(7011) = {7009, 7003};
132 Line(7012) = {7010, 7002};
133 Line(7014) = {7011, 7012};
134 Circle(7015) = {7012, 7016, 7017};
135 Line(7016) = {7017, 7021};
136 Circle(7017) = {7021, 7025, 7011};
137 Circle(7019) = {7029, 7016, 7012};
138 Circle(7021) = {7017, 7016, 7041};
139 Circle(7022) = {7041, 7016, 7029};
140 Line(7024) = {7029, 7050};
141 Circle(7025) = {7050, 7025, 7011};
142 Circle(7030) = {7050, 7025, 7073};
143 Line(7031) = {7073, 7041};

```

```

144 Circle(7035) = {7021, 7025, 7073};
145
146
147 ////////////////////////////////////////////////////
148 //          Surfaces for volume          //
149 //          around bom                   //
150 ////////////////////////////////////////////////////
151
152 Line Loop(7001) = {7004, 7001, 7002, 7003};
153 Plane Surface(7001) = {7001};
154 Line Loop(7002) = {7005, 7006, 7007, 7008};
155 Plane Surface(7002) = {7002};
156 Line Loop(7003) = {7009, -7003, -7012, 7008};
157 Ruled Surface(7003) = {7003};
158 Line Loop(7004) = {7009, 7004, 7010, -7005};
159 Ruled Surface(7004) = {7004};
160 Line Loop(7005) = {7010, 7006, 7011, -7001};
161 Ruled Surface(7005) = {7005};
162 Line Loop(7006) = {7011, 7002, -7012, -7007};
163 Ruled Surface(7006) = {7006};
164 Line Loop(7013) = {7014, 7015, 7016, 7017};
165 Ruled Surface(7013) = {7013};
166 Line Loop(7018) = {7019, 7015, 7021, 7022};
167 Plane Surface(7018) = {7018};
168 Line Loop(7023) = {7024, 7025, 7014, -7019};
169 Ruled Surface(7023) = {7023};
170 Line Loop(7028) = {7024, 7030, 7031, 7022};
171 Ruled Surface(7028) = {7028};
172 Line Loop(7033) = {7016, 7035, 7031, -7021};
173 Ruled Surface(7033) = {7033};
174 Line Loop(7038) = {7025, -7017, 7035, -7030};
175 Plane Surface(7038) = {7038};
176
177
178 ////////////////////////////////////////////////////
179 //          Volume around bom          //
180 ////////////////////////////////////////////////////
181
182 Surface Loop(7039) = {7005, 7004, 7003, 7001, 7006, 7002};
183 Surface Loop(7040) = {7038, 7023, 7028, 7033, 7013, 7018};
184 Volume(7001) = {7039, 7040};
185
186
187 ////////////////////////////////////////////////////
188 //          Points for the SC          //
189 ////////////////////////////////////////////////////
190
191 Point(3001) = {0, 0, 0, cl_sc};
192 Point(3002) = {3.6, 0, 0, cl_sc};
193 Point(3003) = {4.415, 0, 0, cl_sc};
194 Point(3004) = {4.865, 0, 0, cl_sc};
195 Point(3005) = {5.09, 0, 0, cl_sc};
196 Point(3006) = {0, 0.9, 0, cl_sc};
197 Point(3007) = {3.6, 0.9, 0, cl_sc};
198 Point(3008) = {4.415, 1.125, 0, cl_sc};
199 Point(3009) = {4.865, 1.125, 0, cl_sc};
200 Point(3010) = {5.09, 1.125, 0, cl_sc};
201 Point(3011) = {4.865, 0, 1.125, cl_sc};
202 Point(3012) = {5.09, 0, 1.125, cl_sc};
203 Point(3015) = {4.415, 0, 1.125, cl_sc};
204 Point(3019) = {3.6, 0, 0.9, cl_sc};
205 Point(3023) = {0, 0, 0.9, cl_sc};
206 Point(3024) = {4.865, -1.125, 0, cl_sc};
207 Point(3025) = {5.09, -1.125, 0, cl_sc};
208 Point(3028) = {4.415, -1.125, 0, cl_sc};
209 Point(3032) = {3.6, -0.9, 0, cl_sc};
210 Point(3036) = {0, -0.9, 0, cl_sc};
211 Point(3037) = {4.865, 0, -1.125, cl_sc};
212 Point(3038) = {5.09, 0, -1.125, cl_sc};
213 Point(3041) = {4.415, 0, -1.125, cl_sc};
214 Point(3045) = {3.6, 0, -0.9, cl_sc};
215 Point(3049) = {0, 0, -0.9, cl_sc};
216 Point(3050) = {4.865, 1.113819637203975, 0.1582113010464356, cl_sc};
217 Point(3051) = {5.09, 1.113819637203975, 0.1582113010464356, cl_sc};
218 Point(3054) = {4.415, 1.113819637203975, 0.1582113010464356, cl_sc};
219 Point(3058) = {3.6, 0.8910557097631799, 0.1265690408371485, cl_sc};
220 Point(3062) = {0, 0.8910557097631799, 0.1265690408371485, cl_sc};
221 Point(3063) = {4.865, 12.125, 0, cl_int};
222 Point(3064) = {5.09, 12.125, 0, cl_int};
223 Point(3065) = {4.865, 12.125, 0.1582113010464356, cl_int};
224 Point(3066) = {5.09, 12.125, 0.1582113010464356, cl_int};
225 Point(5001) = {6, 0, 0, cl_sc};
226 Point(5002) = {6, 2, 0, cl_sc};

```

```

227 Point(5003) = {6, -2, 0, cl_sc};
228 Point(5004) = {6, 0, 2, cl_sc};
229 Point(5005) = {6, 0, -2, cl_sc};
230 Point(5006) = {5.19, 0, 0, cl_sc};
231
232
233 ///////////////////////////////////////////////////////////////////
234 //          Lines for boundary          //
235 ///////////////////////////////////////////////////////////////////
236
237 Line(2013) = {2012, 2011};
238 Line(2014) = {2011, 2014};
239 Line(2015) = {2014, 2013};
240 Line(2016) = {2013, 2012};
241 Line(2017) = {2012, 2009};
242 Line(2018) = {2009, 2010};
243 Line(2019) = {2010, 2011};
244 Line(2020) = {2009, 2016};
245 Line(2021) = {2016, 2015};
246 Line(2022) = {2015, 2014};
247 Line(2023) = {2013, 2016};
248 Line(2024) = {2015, 2010};
249
250
251 ///////////////////////////////////////////////////////////////////
252 //          Lines for SC          //
253 ///////////////////////////////////////////////////////////////////
254
255 Line(3001) = {3006, 3007};
256 Line(3002) = {3007, 3008};
257 Line(3003) = {3008, 3009};
258 Line(3004) = {3009, 3010};
259 Line(3005) = {3011, 3012};
260 Line(3006) = {3015, 3011};
261 Line(3007) = {3019, 3015};
262 Line(3008) = {3023, 3019};
263 Line(3009) = {3024, 3025};
264 Line(3010) = {3028, 3024};
265 Line(3011) = {3032, 3028};
266 Line(3012) = {3036, 3032};
267 Line(3013) = {3037, 3038};
268 Line(3014) = {3041, 3037};
269 Line(3015) = {3045, 3041};
270 Line(3016) = {3049, 3045};
271 Line(3017) = {3050, 3051};
272 Line(3018) = {3054, 3050};
273 Line(3019) = {3058, 3054};
274 Line(3020) = {3062, 3058};
275 Circle(3021) = {3006, 3001, 3049};
276 Circle(3022) = {3049, 3001, 3036};
277 Circle(3023) = {3036, 3001, 3023};
278 Circle(3024) = {3023, 3001, 3062};
279 Circle(3025) = {3062, 3001, 3006};
280 Circle(3026) = {3007, 3002, 3045};
281 Circle(3027) = {3045, 3002, 3032};
282 Circle(3028) = {3032, 3002, 3019};
283 Circle(3029) = {3019, 3002, 3058};
284 Circle(3030) = {3058, 3002, 3007};
285 Circle(3031) = {3008, 3003, 3041};
286 Circle(3032) = {3041, 3003, 3028};
287 Circle(3033) = {3028, 3003, 3015};
288 Circle(3034) = {3015, 3003, 3054};
289 Circle(3035) = {3054, 3003, 3008};
290 Circle(3036) = {3009, 3004, 3037};
291 Circle(3037) = {3037, 3004, 3024};
292 Circle(3038) = {3024, 3004, 3011};
293 Circle(3039) = {3011, 3004, 3050};
294 Circle(3040) = {3050, 3004, 3009};
295 Circle(3041) = {3010, 3005, 3038};
296 Circle(3042) = {3038, 3005, 3025};
297 Circle(3043) = {3025, 3005, 3012};
298 Circle(3044) = {3012, 3005, 3051};
299 Circle(3045) = {3051, 3005, 3010};
300 Line(3090) = {3063, 3064};
301 Line(3091) = {3064, 3066};
302 Line(3092) = {3066, 3065};
303 Line(3093) = {3065, 3063};
304 Line(3094) = {3010, 14002};
305 Line(3095) = {14001, 3009};
306 Line(3096) = {3050, 14003};
307 Line(3097) = {14004, 3051};
308 Circle(5001) = {5002, 5001, 5005};
309 Circle(5002) = {5005, 5001, 5003};

```

```

310 Circle(5003) = {5003, 5001, 5004};
311 Circle(5004) = {5004, 5001, 5002};
312 Ellipse(5005) = {5005, 5001, 5006, 5006};
313 Ellipse(5006) = {5002, 5001, 5006, 5006};
314 Ellipse(5007) = {5004, 5001, 5006, 5006};
315 Ellipse(5008) = {5003, 5001, 5006, 5006};
316 Line(5025) = {5007, 5008};
317 Line(5026) = {5008, 5012};
318 Line(5027) = {5012, 5016};
319 Line(5028) = {5016, 5007};
320 Line(5031) = {5008, 5028};
321 Line(5032) = {5028, 5032};
322 Line(5033) = {5032, 5007};
323 Line(5036) = {5032, 5044};
324 Line(5037) = {5044, 5048};
325 Line(5038) = {5048, 5028};
326 Line(5041) = {5016, 5044};
327 Line(5043) = {5048, 5012};
328 Line(90003) = {3066, 14004};
329 Line(90004) = {3064, 14002};
330 Line(90005) = {3063, 14001};
331 Line(90006) = {3065, 14003};
332 Line(90028) = {14005, 14006};
333 Line(90029) = {14006, 14010};
334 Line(90030) = {14010, 14014};
335 Line(90031) = {14014, 14005};
336 Line(90034) = {14010, 14026};
337 Line(90035) = {14026, 14030};
338 Line(90036) = {14030, 14006};
339 Line(90038) = {14030, 14038};
340 Line(90039) = {14038, 14042};
341 Line(90040) = {14042, 14026};
342 Line(90044) = {14005, 14038};
343 Line(90046) = {14042, 14014};
344
345
346 ////////////////////////////////////////////////////
347 //          Surface boundary          //
348 ////////////////////////////////////////////////////
349
350 Line Loop(2025) = {2013, -2019, -2018, -2017};
351 Plane Surface(2025) = {2025};
352 Line Loop(2026) = {2015, 2023, 2021, 2022};
353 Plane Surface(2026) = {2026};
354 Line Loop(2027) = {2016, 2017, 2020, -2023};
355 Plane Surface(2027) = {2027};
356 Line Loop(2028) = {2016, 2013, 2014, 2015};
357 Plane Surface(2028) = {2028};
358 Line Loop(2029) = {2014, -2022, 2024, 2019};
359 Plane Surface(2029) = {2029};
360 Line Loop(2030) = {2020, 2021, 2024, -2018};
361 Plane Surface(2030) = {2030};
362
363
364 ////////////////////////////////////////////////////
365 //          Surface inner volume      //
366 ////////////////////////////////////////////////////
367
368 Line Loop(2031) = {5025, 5026, 5027, 5028, -14005, -14008, -14007, -14006};
369 Plane Surface(2031) = {2031};
370 Line Loop(2032) = {5025, 5031, 5032, 5033};
371 Plane Surface(2032) = {2032};
372 Line Loop(2033) = {5032, 5036, 5037, 5038};
373 Plane Surface(2033) = {2033};
374 Line Loop(2034) = {5027, 5041, 5037, 5043};
375 Plane Surface(2034) = {2034};
376 Line Loop(2035) = {5026, -5043, 5038, -5031};
377 Plane Surface(2035) = {2035};
378 Line Loop(2036) = {5028, -5033, 5036, -5041};
379 Plane Surface(2036) = {2036};
380
381
382 ////////////////////////////////////////////////////
383 //          Surface SC                //
384 ////////////////////////////////////////////////////
385
386 Line Loop(3047) = {3025, 3021, 3022, 3023, 3024};
387 Plane Surface(3047) = {3047};
388 Line Loop(3049) = {3041, 3042, 3043, 3044, 3045};
389 Plane Surface(3049) = {3049};
390 Line Loop(3051) = {3020, -3029, -3008, 3024};
391 Ruled Surface(3051) = {3051};
392 Line Loop(3053) = {3020, 3030, -3001, -3025};

```

```

393 Ruled Surface(3053) = {3053};
394 Line Loop(3055) = {3026, -3016, -3021, 3001};
395 Ruled Surface(3055) = {3055};
396 Line Loop(3057) = {3016, 3027, -3012, -3022};
397 Ruled Surface(3057) = {3057};
398 Line Loop(3059) = {3012, 3028, -3008, -3023};
399 Ruled Surface(3059) = {3059};
400 Line Loop(3061) = {3034, -3019, -3029, 3007};
401 Ruled Surface(3061) = {3061};
402 Line Loop(3063) = {3035, -3002, -3030, 3019};
403 Ruled Surface(3063) = {3063};
404 Line Loop(3065) = {3031, -3015, -3026, 3002};
405 Ruled Surface(3065) = {3065};
406 Line Loop(3067) = {3015, 3032, -3011, -3027};
407 Ruled Surface(3067) = {3067};
408 Line Loop(3069) = {3028, 3007, -3033, -3011};
409 Ruled Surface(3069) = {3069};
410 Line Loop(3071) = {3003, 3036, -3014, -3031};
411 Ruled Surface(3071) = {3071};
412 Line Loop(3073) = {3014, 3037, -3010, -3032};
413 Ruled Surface(3073) = {3073};
414 Line Loop(3075) = {3010, 3038, -3006, -3033};
415 Ruled Surface(3075) = {3075};
416 Line Loop(3077) = {3006, 3039, -3018, -3034};
417 Ruled Surface(3077) = {3077};
418 Line Loop(3079) = {3018, 3040, -3003, -3035};
419 Ruled Surface(3079) = {3079};
420 Line Loop(3081) = {3004, 3041, -3013, -3036};
421 Ruled Surface(3081) = {3081};
422 Line Loop(3083) = {3042, -3009, -3037, 3013};
423 Ruled Surface(3083) = {3083};
424 Line Loop(3085) = {3043, -3005, -3038, 3009};
425 Ruled Surface(3085) = {3085};
426 Line Loop(3087) = {3039, 3017, -3044, -3005};
427 Ruled Surface(3087) = {3087};
428 Line Loop(3099) = {3090, 3091, 3092, 3093};
429 Plane Surface(3099) = {3099};
430 Line Loop(5010) = {5006, -5005, -5001};
431 Ruled Surface(5010) = {5010};
432 Line Loop(5012) = {5005, -5008, -5002};
433 Ruled Surface(5012) = {5012};
434 Line Loop(5014) = {5008, -5007, -5003};
435 Ruled Surface(5014) = {5014};
436 Line Loop(5016) = {5007, -5006, -5004};
437 Ruled Surface(5016) = {5016};
438 Line Loop(5018) = {5004, 5001, 5002, 5003};
439 Plane Surface(5018) = {5018};
440 Line Loop(90008) = {3092, 90006, 14006, -90003};
441 Plane Surface(90008) = {90008};
442 Line Loop(90010) = {90003, 14007, -90004, 3091};
443 Plane Surface(90010) = {90010};
444 Line Loop(90012) = {3090, 90004, 14008, -90005};
445 Plane Surface(90012) = {90012};
446 Line Loop(90014) = {90005, 14005, -90006, 3093};
447 Plane Surface(90014) = {90014};
448 Line Loop(90016) = {3096, -14005, 3095, -3040};
449 Plane Surface(90016) = {90016};
450 Line Loop(90018) = {14006, 3097, -3017, 3096};
451 Plane Surface(90018) = {90018};
452 Line Loop(90020) = {14007, -3094, -3045, -3097};
453 Plane Surface(90020) = {90020};
454 Line Loop(90022) = {3094, 14008, 3095, 3004};
455 Plane Surface(90022) = {90022};
456
457
458 ////////////////////////////////////////////////////
459 // Surface for the intermediate volume //
460 ////////////////////////////////////////////////////
461
462 Line Loop(90027) = {90028, 90029, 90030, 90031};
463 Plane Surface(90027) = {90027};
464 Line Loop(90032) = {90029, 90034, 90035, 90036};
465 Plane Surface(90032) = {90032};
466 Line Loop(90037) = {90038, 90039, 90040, 90035};
467 Plane Surface(90037) = {90037};
468 Line Loop(90042) = {90031, 90044, 90039, 90046};
469 Plane Surface(90042) = {90042};
470 Line Loop(90047) = {90028, -90036, 90038, -90044};
471 Plane Surface(90047) = {90047};
472 Line Loop(90052) = {90030, -90046, 90040, -90034};
473 Plane Surface(90052) = {90052};
474
475

```

```

476 ////////////////////////////////////////////////////
477 // Volume for inner box excluding SC //
478 // and volume around bom. //
479 ////////////////////////////////////////////////////
480
481 Surface Loop(90053) = {2031, 2032, 2035, 2034, 2036, 2033, 3051, 3053, 3063, 3079, 3077, 3075, 3073, 3071, 3081, 90022, 90020,
482 3049, 3083, 3085, 3087, 90018, 90016, 3065, 3067, 3069, 3059, 3057, 3055, 3047, 3061};
483 Surface Loop(90054) = {5010, 5016, 5014, 5012, 5018};
484 Volume(90055) = {90053, 90054, 7039};
485
486
487 ////////////////////////////////////////////////////
488 // Volume for intermid. box excluding //
489 // inner volume and bom. //
490 ////////////////////////////////////////////////////
491
492 Surface Loop(90056) = {90027, 90047, 90032, 90052, 90042, 90037};
493 Surface Loop(90057) = {90012, 3099, 90010, 90008, 90014, 2031, 2032, 2035, 2034, 2036, 2033};
494 Volume(90058) = {90056, 90057};
495
496
497 ////////////////////////////////////////////////////
498 // Volume for outer box excluding //
499 // intermediate volume. //
500 ////////////////////////////////////////////////////
501
502 Surface Loop(90059) = {2028, 2027, 2025, 2029, 2026, 2030};
503 Volume(90060) = {90059, 90056};
504
505
506 ////////////////////////////////////////////////////
507 // Physicals to be used by SPIS //
508 ////////////////////////////////////////////////////
509
510 // Outer boundary, ID = 2001
511 Physical Surface(2001) = {2025, 2026, 2027, 2028, 2029, 2030};
512
513 // SC surface, ID = 3002
514 Physical Surface(3002) = {3047, 3049, 3051, 3053, 3055, 3057, 3059, 3061, 3063, 3065, 3067, 3069, 3071, 3073, 3075, 3077, 3079,
515 3081, 3083, 3085, 3087, 3099, 5010, 5012, 5014, 5016, 5018, 7038, 7023, 7013, 7033, 7028, 7018, 90008, 90010, 90012, 90014,
516 90016, 90018, 90020, 90022};
517
518 // Plasma volume, ID = 6001
519 Physical Volume(6001) = {7001, 90055, 90058, 90060};

```

---

Please note that the lines 481 and 514 have been split up to fit inside this document, in the model file however they must be continuous.

## B.2 Langmuir probe model

```
LP_Stub.geo
1 ////////////////////////////////////////////////////////////////////
2 // Copyright Thomas Nilsson //
3 ////////////////////////////////////////////////////////////////////
4 ////////////////////////////////////////////////////////////////////
5 // Parameters for the mesh //
6 ////////////////////////////////////////////////////////////////////
7
8 cl_probe = 0.005;
9 cl_inner = 0.01;
10 cl_intermid = 0.07;
11 cl_boundary = 0.4;
12
13
14 ////////////////////////////////////////////////////////////////////
15 // Points for LP with stub //
16 ////////////////////////////////////////////////////////////////////
17
18 Point(1) = {0.209, 0, 0, cl_probe};
19 Point(2) = {0.234, 0, 0, cl_probe};
20 Point(3) = {0.259, 0, 0, cl_probe};
21 Point(4) = {0.209202432074906, 0, 0.00317500000005611, cl_probe};
22 Point(5) = {0.209202432074906, 0, -0.00317500000005611, cl_probe};
23 Point(6) = {0.209202432074906, 0.00317500000005611, 0, cl_probe};
24 Point(7) = {0.209202432074906, -0.00317500000005611, 0, cl_probe};
25 Point(8) = {0.234, 0, 0.025, cl_probe};
26 Point(9) = {0.234, 0, -0.025, cl_probe};
27 Point(10) = {0.234, -0.025, 0, cl_probe};
28 Point(11) = {0.234, 0.025, 0, cl_probe};
29 Point(12) = {0.209202432074906, 0, 0, cl_probe};
30 Point(13) = {0.1, 0, -0.003175, cl_probe};
31 Point(14) = {0.1, 0, 0, cl_probe};
32 Point(15) = {0.1, 0.003175, 0, cl_probe};
33 Point(16) = {0.1, 0, 0.003175, cl_probe};
34 Point(17) = {0.1, -0.003175, 0, cl_probe};
35
36
37 ////////////////////////////////////////////////////////////////////
38 // Points for inner volume //
39 ////////////////////////////////////////////////////////////////////
40
41 Point(18) = {0.1, 0.05, 0, cl_inner};
42 Point(19) = {0.1, -0.05, 0, cl_inner};
43 Point(20) = {0.1, 0, 0.05, cl_inner};
44 Point(21) = {0.1, 0, -0.05, cl_inner};
45 Point(22) = {0.309, 0, 0.05, cl_inner};
46 Point(23) = {0.309, 0, 0, cl_inner};
47 Point(24) = {0.309, 0.05, 0, cl_inner};
48 Point(25) = {0.309, -0.05, 0, cl_inner};
49 Point(26) = {0.309, 0, -0.05, cl_inner};
50
51
52 ////////////////////////////////////////////////////////////////////
53 // Points interface between parts //
54 // of stub in and out of shade. //
55 // For future use only //
56 ////////////////////////////////////////////////////////////////////
57
58 Point(27) = {0.160905, 0, 0, cl_probe};
59 Point(28) = {0.160905, 0, -0.003175, cl_probe};
60 Point(29) = {0.160905, 0.003175, 0, cl_probe};
61 Point(30) = {0.160905, 0, 0.003175, cl_probe};
62 Point(31) = {0.160905, -0.003175, 0, cl_probe};
63
64
65 ////////////////////////////////////////////////////////////////////
66 // Points for intermediate volume //
67 ////////////////////////////////////////////////////////////////////
68
69 Point(32) = {-0.2, 0, 0, cl_intermid};
70 Point(33) = {-0.2, 0.225, 0, cl_intermid};
71 Point(34) = {-0.2, -0.225, 0, cl_intermid};
72 Point(35) = {-0.2, 0, 0.225, cl_intermid};
73 Point(36) = {-0.2, 0, -0.225, cl_intermid};
74 Point(37) = {0.459, 0, 0.225, cl_intermid};
75 Point(38) = {0.459, 0, 0, cl_intermid};
76 Point(39) = {0.459, 0.225, 0, cl_intermid};
77 Point(40) = {0.459, -0.225, 0, cl_intermid};
78 Point(41) = {0.459, 0, -0.225, cl_intermid};
79
80
```



```

81 ////////////////////////////////////////////////////
82 //           Points for outer boundary           //
83 ////////////////////////////////////////////////////
84
85 Point(42) = {-0.3, 0, 0, cl_boundary};
86 Point(43) = {-0.3, 1.025, 0, cl_boundary};
87 Point(44) = {-0.3, -1.025, 0, cl_boundary};
88 Point(45) = {-0.3, 0, 1.025, cl_boundary};
89 Point(46) = {-0.3, 0, -1.025, cl_boundary};
90 Point(47) = {1.259, 0, 1.025, cl_boundary};
91 Point(48) = {1.259, 0, 0, cl_boundary};
92 Point(49) = {1.259, 1.025, 0, cl_boundary};
93 Point(50) = {1.259, -1.025, 0, cl_boundary};
94 Point(51) = {1.259, 0, -1.025, cl_boundary};
95
96
97 ////////////////////////////////////////////////////
98 //           Circles and lines           //
99 ////////////////////////////////////////////////////
100
101 Circle (1) = {3, 2, 8};
102 Circle (2) = {5, 2, 9};
103 Circle (3) = {9, 2, 3};
104 Circle (4) = {3, 2, 10};
105 Circle (5) = {9, 2, 10};
106 Circle (6) = {10, 2, 8};
107 Circle (7) = {8, 2, 11};
108 Circle (8) = {11, 2, 9};
109 Circle (9) = {3, 2, 11};
110 Circle (10) = {11, 2, 6};
111 Circle (11) = {7, 2, 10};
112 Circle (12) = {8, 2, 4};
113 Circle (13) = {6, 12, 4};
114 Circle (14) = {4, 12, 7};
115 Circle (15) = {7, 12, 5};
116 Circle (16) = {5, 12, 6};
117 Circle (17) = {13, 14, 15};
118 Circle (18) = {15, 14, 16};
119 Circle (19) = {16, 14, 17};
120 Circle (20) = {17, 14, 13};
121 Line (21) = {15, 29};
122 Line (22) = {13, 28};
123 Line (23) = {17, 31};
124 Line (24) = {30, 16};
125 Circle (25) = {18, 14, 21};
126 Circle (26) = {21, 14, 19};
127 Circle (27) = {19, 14, 20};
128 Circle (28) = {20, 14, 18};
129 Circle (29) = {22, 23, 24};
130 Circle (30) = {25, 23, 22};
131 Circle (31) = {24, 23, 26};
132 Circle (32) = {26, 23, 25};
133 Line (33) = {26, 21};
134 Line (34) = {18, 24};
135 Line (35) = {22, 20};
136 Line (36) = {19, 25};
137 Circle (37) = {28, 27, 29};
138 Circle (38) = {29, 27, 30};
139 Circle (39) = {30, 27, 31};
140 Circle (40) = {31, 27, 28};
141 Line (41) = {29, 6};
142 Line (42) = {28, 5};
143 Line (43) = {31, 7};
144 Line (44) = {4, 30};
145 Circle (45) = {33, 32, 36};
146 Circle (46) = {36, 32, 34};
147 Circle (47) = {34, 32, 35};
148 Circle (48) = {35, 32, 33};
149 Circle (49) = {37, 38, 40};
150 Circle (50) = {40, 38, 41};
151 Circle (51) = {41, 38, 39};
152 Circle (52) = {39, 38, 37};
153 Line (53) = {36, 41};
154 Line (54) = {34, 40};
155 Line (55) = {35, 37};
156 Line (56) = {33, 39};
157 Circle (57) = {43, 42, 46};
158 Circle (58) = {46, 42, 44};
159 Circle (59) = {44, 42, 45};
160 Circle (60) = {45, 42, 43};
161 Circle (61) = {47, 48, 50};
162 Circle (62) = {50, 48, 51};
163 Circle (63) = {51, 48, 49};

```

```

164 Circle (64) = {49, 48, 47};
165 Line (65) = {46, 51};
166 Line (66) = {44, 50};
167 Line (67) = {45, 47};
168 Line (68) = {43, 49};
169
170
171 ////////////////////////////////////////////////////////////////////
172 //          Surfaces          //
173 ////////////////////////////////////////////////////////////////////
174
175 Line Loop (1) = {40, -22, -20, 23};
176 Ruled Surface (1) = {1};
177 Line Loop (2) = {22, 37, -21, -17};
178 Ruled Surface (2) = {2};
179 Line Loop (3) = {38, 24, -18, 21};
180 Ruled Surface (3) = {3};
181 Line Loop (4) = {23, -39, 24, 19};
182 Ruled Surface (4) = {4};
183 Line Loop (5) = {15, 2, 5, -11};
184 Ruled Surface (5) = {5};
185 Line Loop (6) = {2, -8, 10, -16};
186 Ruled Surface (6) = {6};
187 Line Loop (7) = {11, 6, 12, 14};
188 Ruled Surface (7) = {7};
189 Line Loop (8) = {10, 13, -12, 7};
190 Ruled Surface (8) = {8};
191 Line Loop (9) = {1, 7, -9};
192 Ruled Surface (9) = {9};
193 Line Loop (10) = {1, -6, -4};
194 Ruled Surface (10) = {10};
195 Line Loop (11) = {4, -5, 3};
196 Ruled Surface (11) = {11};
197 Line Loop (12) = {3, 9, 8};
198 Ruled Surface (12) = {12};
199 Line Loop (13) = {29, 31, 32, 30};
200 Plane Surface (13) = {13};
201 Line Loop (14) = {29, -34, -28, -35};
202 Ruled Surface (14) = {14};
203 Line Loop (15) = {35, -27, 36, 30};
204 Ruled Surface (15) = {15};
205 Line Loop (16) = {36, -32, 33, 26};
206 Ruled Surface (16) = {16};
207 Line Loop (17) = {34, 31, 33, -25};
208 Ruled Surface (17) = {17};
209 Line Loop (18) = {13, 44, -38, 41};
210 Ruled Surface (18) = {18};
211 Line Loop (19) = {14, -43, -39, -44};
212 Ruled Surface (19) = {19};
213 Line Loop (20) = {15, -42, -40, 43};
214 Ruled Surface (20) = {20};
215 Line Loop (21) = {16, -41, -37, 42};
216 Ruled Surface (21) = {21};
217 Line Loop (22) = {46, 47, 48, 45};
218 Plane Surface (22) = {22};
219 Line Loop (23) = {50, 51, 52, 49};
220 Plane Surface (23) = {23};
221 Line Loop (24) = {53, 51, -56, 45};
222 Ruled Surface (24) = {24};
223 Line Loop (25) = {56, 52, -55, 48};
224 Ruled Surface (25) = {25};
225 Line Loop (26) = {49, -54, 47, 55};
226 Ruled Surface (26) = {26};
227 Line Loop (27) = {50, -53, 46, 54};
228 Ruled Surface (27) = {27};
229 Line Loop (28) = {58, 59, 60, 57};
230 Plane Surface (28) = {28};
231 Line Loop (29) = {62, 63, 64, 61};
232 Plane Surface (29) = {29};
233 Line Loop (30) = {65, 63, -68, 57};
234 Ruled Surface (30) = {30};
235 Line Loop (31) = {68, 64, -67, 60};
236 Ruled Surface (31) = {31};
237 Line Loop (32) = {61, -66, 59, 67};
238 Ruled Surface (32) = {32};
239 Line Loop (33) = {62, -65, 58, 66};
240 Ruled Surface (33) = {33};
241 Line Loop (34) = {18, 19, 20, 17};
242 Plane Surface (34) = {34};
243 Line Loop (35) = {25, 26, 27, 28, 20, 17, 18, 19};
244 Plane Surface (35) = {35};
245
246

```

```

247 ////////////////////////////////////////////////////
248 //           Volumes           //
249 ////////////////////////////////////////////////////
250
251 // Inner volume, excluding the LP with sphere and stub
252 Surface Loop (1) = {14, 13, 17, 16, 15, 35, 6, 5, 20, 21, 18, 8, 7, 10, 9, 12, 11, 19, 4, 1, 2, 3};
253 Volume (1) = {1};
254
255 // Intermediate volume, excluding inner volume
256 Surface Loop (2) = {26, 23, 27, 24, 25, 22, 35, 17, 14, 13, 16, 15, 34};
257 Volume (2) = {2};
258
259 // Outer volume, excluding intermediate volume
260 Surface Loop (3) = {32, 29, 33, 30, 31, 28, 26, 23, 27, 24, 25, 22};
261 Volume (3) = {3};
262
263
264 ////////////////////////////////////////////////////
265 //           Physicals to be used by SPIS           //
266 ////////////////////////////////////////////////////
267
268 // Outer boundary, ID = 2001
269 Physical Surface (2001) = {28, 29, 30, 31, 32, 33};
270
271 // LP sphere, ID = 3001
272 Physical Surface (3001) = {5, 6, 7, 8, 9, 10, 11, 12};
273
274 // LP stub, ID = 3002
275 Physical Surface (3002) = {1, 2, 3, 4, 18, 19, 20, 21};
276
277 // LP bottom of stub, ID = 3003
278 Physical Surface (3003) = {34};
279
280 // Plasma volume, ID = 6001
281 Physical Volume (6001) = {1, 2, 3};

```

---

Please note that this model have to be modified manually (by changing the characteristic lengths and simulation box size) depending on the Debye length of the plasma simulated.

## **Appendix C**

### **Appendix: List of simulations**

Here follows a short list of all the simulations used in this report, beginning with the simulations of the Cassini spacecraft.

Plasmas for the Cassini spacecraft simulations										
Debye length (m)	n (per cubic cm)	T (eV)	Avg.part/cell	Time (ms)	Capacitance (nF)	Model file	Usc (V)	U1/Usc		
0.235	100	0.1	7.4	8.5	1.0	Case A	-0.3059	0.282		
0.743	100 10	1 0.1	5.0	10.0	1.0	Case B	-2.9511 -0.2955	0.446 0.448		
2.35	100 10 1	10 1 0.1	8.9	1.8 1.5 10.0	0.5 0.5 0.2	Case C	-29.1138 -2.7426 -0.2889	0.611 0.607 0.607		
7.43	10 1 0.1	10 1 0.1	7.6	1.0 10.0 10.0	0.1 0.1 0.15	Case D	-25.3565 -2.5629 -0.2451	0.688 0.690 0.687		
23.5	1 0.1 0.01	10 1 0.1	8.4	10.0 10.0 50.0	0.1 0.5 0.08	Case E	-25.3487 -2.5079 -0.2380	0.741 0.739 0.759		
74.3	0.1 0.01	10 1	9.3	10.0	0.01	Case F	-25.3514 -2.2923	0.760 0.761		

**Table C.1:** The various plasmas and settings used in the simulations with the Cassini spacecraft. Together with the results,  $U_{sc}$  corresponds to the spacecraft potential and  $U1/U_{sc}$  is the ratio of the remaining spacecraft potential at the position where the Langmuir probe would be. The models for each specific Debye length can be found on [http://www.space.irfu.se/exjobb/2009\\_thomas\\_nilsson/](http://www.space.irfu.se/exjobb/2009_thomas_nilsson/).

Current collected to the Langmuir probe, OML-case				
Density (per cubic cm)	Temperature (eV)	Time (ms)	Electron speedup	
1	1	1.5	1	
Number of tetrahedrons		Macroparticles (for each species)		
≈ 45,000		≈ 600,000		
Potential (V)	Sphere current (nA)	OML current (nA)	Current to LP (nA)	Current to stub (nA)
-7	-	-0.0391	-0.0473	-0.0108
-6	-	-0.0339	-0.0406	-0.0092
-5	-0.0353	-0.0281	-0.0325	-0.0079
-4	-0.0258	-0.0207	-0.0226	-0.0063
-3	-0.0152	-0.0092	-0.0096	-0.0034
-2	0.0121	0.0138	0.0136	0.0005
-1	0.0639	0.0676	0.0680	0.0159
0	0.2003	0.2056	0.2011	0.0502
0.5	0.3046	0.3128	0.2903	0.0794
1	0.4093	0.4193	0.4035	0.0999
1.5	-	0.5252	0.4917	0.1192
2	0.6194	0.6309	0.5889	0.1487
2.5	-	0.7365	0.6931	0.1668
3	0.8317	0.8419	0.7926	0.1934
4	1.0504	1.0526	1.0023	0.2410
5	1.2606	1.2632	1.2117	0.2893
6	1.4773	1.4737	-	-
7	1.6860	1.6842	-	-
8	1.8952	1.8948	-	-
9	2.0999	2.1053	-	-
10	2.3157	2.3158	2.2376	1.8057
15	3.3893	3.3685	-	-
20	4.4532	4.4212	4.2964	3.4371
25	5.5240	5.4738	-	-
28	6.1358	6.1054	6.0368	1.452

**Table C.2:** *The current flow to the various parts of the Langmuir probe used for the sweep in the low density and high temperature plasma. (In which OML-theory is valid). The sphere is the control, without the stub present and the LP is the sphere of the Langmuir probe with the stub present. The current to the stub is listed here, for comparison, even though it is not measured by the actual instrument. The boundary cylinder had a radius of about 15 meters and a length of approximately 30 meters.*

Current collected to the Langmuir probe, high density-case			
Density (per cubic cm)	Temperature (eV)	Time (ms)	Electron speedup
1,000	0.05	0.5	42
Number of tetrahedrons		Macroparticles (for each species)	
≈ 160,000		≈ 750,000	
Potential (V)	Current to sphere (nA)	Current to LP (nA)	Current to stub (nA)
-0.2	-4.324	-4.328	-0.933
-0.1	2.850	2.510	1.117
0	42.460	42.385	11.434
0.1	132.44	128.79	30.166
0.2	221.56	211.74	47.086
0.5	484.38	458.21	94.409
0.7	654.75	613.44	124.87
1	905.75	843.66	168.29
Potential (V)	Electron speedup	Current to LP (nA)	Current to stub (nA)
1	1 (as control)	823.52	164.15
Coordinates for model used, stub along x-axis, (m)			
Boundary cylinder	Intermediate cylinder	Inner cylinder	LP and stub
<b>x:</b> -0.1 to 0.55	0.08 to 0.329	0.1 to 0.309	0.1 to 0.259
<b>radius (y&amp;z):</b> 0.4	0.1	0.05	0.025
<b>Char.length:</b> 0.0262	0.024	0.01	0.01

**Table C.3:** *The current flow to the various parts of the Langmuir probe used for the sweep in the high density and low temperature plasma. (In which OML-theory is not expected to be valid). The sphere is the control, without the stub present and the LP is the sphere of the Langmuir probe with the stub present. The current to the stub is listed here, for comparison, even though it is not measured by the actual instrument. As the electron speedup factor had to be changed for this sweep one simulation is done with electron speedup equal to one. (same as for the OML-case) The simulation with electron speedup factor equal to one took three days to perform and does not differ to much from the corresponding simulation with electron speedup factor 42. The characteristic lengths varied from 0.01 m on the probe and inner most volume to 0.0262 m at the boundary. The simulation box had the form of a cylinder with radius 0.4 m and length 0.65 m in this simulation where the probe is centred around the point (0.234, 0, 0) and the stub is alongside the negative x-axis.*